

1-1-2009

Accurate Cylindrical-Coordinate Numerical Models For The Analysis Of Hydrologic Tests

John Edward Keller

Southern Illinois University Carbondale, jkeller@siu.edu

Follow this and additional works at: <http://opensiuc.lib.siu.edu/dissertations>

Recommended Citation

Keller, John Edward, "Accurate Cylindrical-Coordinate Numerical Models For The Analysis Of Hydrologic Tests" (2009).
Dissertations. Paper 57.

This Open Access Dissertation is brought to you for free and open access by the Theses and Dissertations at OpenSIUC. It has been accepted for inclusion in Dissertations by an authorized administrator of OpenSIUC. For more information, please contact opensiuc@lib.siu.edu.

**ACCURATE CYLINDRICAL-COORDINATE NUMERICAL
MODELS FOR THE ANALYSIS OF HYDROLOGIC TESTS**

By

John E. Keller

B.S., University of Kansas, 1996

M.S., Southern Illinois University @ Carbondale, 2000

A Dissertation

Submitted in Partial Fulfillment of the Requirements for the
Doctor of Philosophy

Environmental Resources and Policy
in the Graduate School
Southern Illinois University Carbondale
August 2009

DISSERTATION APPROVAL

ACCURATE CYLINDRICAL-COORDINATE NUMERICAL MODELS
FOR THE ANALYSIS OF HYDROLOGIC TESTS

By

John E. Keller

A Dissertation Submitted in Partial

Fulfillment of the Requirements

for the Degree of

Doctor of Philosophy

Environmental Resources and Policy

Approved by:

Dr. Steven Esling, Chair, Department Chair, Geology

Dr. Ken Anderson, Professor, Geology

Dr. Lizette Chevalier, Professor, Engineering

Dr. Bruce Devantier, Professor, Engineering

Dr. Benedy Dziegielewski, Professor, Geography

Graduate School
Southern Illinois University Carbondale
May 13, 2009

AN ABSTRACT OF THE DISSERTATION OF

John Keller, for the Doctor of Philosophy degree in Environmental Resources and Policy, presented on May 13, 2009, at Southern Illinois University Carbondale.

TITLE: ACCURATE CYLINDRICAL-COORDINATE NUMERICAL MODELS
FOR THE ANALYSIS OF HYDROLOGIC TESTS

MAJOR PROFESSOR: Dr. Steven Esling

Analytical solutions to well hydraulic problems have restrictive assumptions that often do not match real world conditions. Although numerical models more closely match reality, they either ran too slowly to be practical or lacked accuracy because of coarse grid spacing and large time steps. Advances in computer power over the last few decades now allow for accurate, fast numerical models that handle complex flow systems. The purpose of this dissertation was to develop flexible and accurate numerical modeling codes for the simulation of hydrologic tests.

One of these numerical modeling codes, the Slug Test Simulator (STS), was designed for the mechanics of a single well test, or slug test. STS can handle a variety of conditions including unconfined flow, partial penetration, layered heterogeneities, and the presence of a homogeneous well skin like existing codes. This program also extends on the capabilities of earlier codes with its ability to simulate a heterogeneous skin where K can vary in both the radial and vertical directions. STS has a clear user interface, can display graphical results, and allows the user to determine hydraulic conductivity through a trial-and-error curve-matching process. Comparisons of STS to the Cooper-Bredehoeft-Papadopoulos analytical solution and the Kansas Geological Survey (KGS) semi-analytical solution produced near-identical curves under a wide variety of conditions.

Numerous analytical studies have shown that the well skin is an important factor in the underestimation of hydraulic conductivity in slug tests. STS allows for the exploration of the well skin issue under conditions too complex for analytical models. Model trials revealed two key discoveries: 1) if any layers within the skin have the same hydraulic conductivity as the surrounding formation, flow is concentrated within these conduits and the resultant head response approaches the case when no skin is present; and 2) the two most important properties in determining the overall influence of the skin are specific storage and skin thickness. The first discovery suggests that extensive development activities can essentially eliminate any well skin impacts. Other factors such as partial penetration, the placement of the well screen, and anisotropy play insignificant roles in resultant head responses.

Recent research is focusing on alternative direct- push (DP) methodologies to determine hydrologic properties. DP offers advantages over traditional well tests, but may yield inaccurate results if the screen becomes clogged during pushing activities. The Kansas Geological Survey (KGS) developed a new DP technique, the Direct-Push Permeameter (DPP), to overcome this limitation. Existing analytical or numerical models cannot address the specialized nature of DPP tests so a second numerical modeling code, the Direct Push Permeameter Simulator (DPSS), was developed. DPSS was generated by modifying STS so both numerical codes are similar in many ways, particularly with their flexibility and accuracy. The codes differ in how they handle vertical layering, the boundary conditions at the well, and the spreadsheet interfaces. DPSS was able to produce near-identical curves in comparison to the Theis analytical solution. DPSS was also able to reasonably recreate DPP field data conducted at two sites with distinctly

different media properties. The GEMS and Nauen sites had an average error of 14.2% and 3.1%, respectively between the field data and DPPS simulations.

ACKNOWLEDGMENTS

I would like to thank my committee members; Dr. Ken Anderson, Dr. Lizette Chevalier, Dr. Bruce Devantier, and Dr. Benedy Dziegielewski. Special thanks go to Dr. Steven Esling, who helped me overcome my fear of writing Visual Basic code. Without his guidance and expertise, I never would have finished so I owe him a great debt. I would also like to thank my high school chemistry teacher, Mrs. Fink, who helped me to discover the scientist and teacher within. Lastly, I would like to thank my parents, Carolyn Brown and George Keller, but special thanks go to my mother whose support over the years was instrumental in finishing my doctoral degree.

TABLE OF CONTENTS

ABSTRACT.....	i
ACKNOWLEDGMENTS	iv
LIST OF TABLES.....	vii
LIST OF FIGURES	viii
CHAPTERS	
CHAPTER 1 – INTRODUCTION.....	1
BACKGROUND	2
OBJECTIVES.....	3
PREVIOUS WORK	
Analytical Studies.....	5
Numerical Studies.....	12
CHAPTER 2 – SLUG TEST SIMULATOR (STS)	14
DERIVATION OF GOVERNING EQUATION	14
CYLINDRICAL FINITE-DIFFERENCE MODELING CODE.....	20
Cylinder Spacing.....	20
Well Skin	22
Boundary Conditions	23
User Interface.....	25
Comparison of Model Features.....	27
MODEL VALIDATION	29
CHAPTER 3 – WELL SKIN.....	34
NUMERICAL MODEL TRIALS.....	34

Specific Storage	35
Well Skin Characteristics.....	36
Partial Penetration.....	44
Anisotropy.....	46
CHAPTER 4 – DIRECT PUSH PERMEAMETER SIMULATOR (DPPS) ...	49
CYLINDRICAL FINITE-DIFFERENCE MODELING CODE	49
DPPS versus STS	49
User Interface.....	52
Comparison of Model Features.....	53
MODEL VALIDATION	55
DPP FIELD DATA COMPARISON.....	57
MODEL ANALYSIS	
Sensitivity Analysis	58
Accuracy Analysis	59
CHAPTER 5 – CONCLUSIONS	62
REFERENCES	67
APPENDICES	
APPENDIX A – STS Visual Basic Code	76
APPENDIX B – DPPS Visual Basic Code.....	97
VITA	113

LIST OF TABLES

<u>TABLE</u>		<u>PAGE</u>
Table 1	Parameter values used in the comparison of STS to the KGS analytical solution.	31
Table 2	Specific storage values used in STS trials	35
Table 3	Parameter values used in anisotropy STS trials	46-47
Table 4	Comparison of DPSS results to field data.....	58
Table 5	Effects of tolerance on DPPS accuracy	60
Table 6	Effects of the number of time steps on DPPS accuracy.....	61

LIST OF FIGURES

<u>FIGURE</u>		<u>PAGE</u>
Figure 1	Cross-sectional view of a hypothetical aquifer used for model derivation	16
Figure 2	Conceptual model showing the design of STS	21
Figure 3	Diagram of the rewetting feature used in STS to handle both falling and rising water tables under unconfined conditions.....	24
Figure 4	STS spreadsheet interface for data entry	25
Figure 5	Normalized head versus time plots of STS compared to the CBP analytical model.....	30
Figure 6	Normalized head versus time plots of STS compared to the KGS semi-analytical model.....	32
Figure 7	Normalized head versus time plots generated by the two specific storage end members.....	36
Figure 8	Normalized head versus time plots showing the effects of both positive and negative well skins	37
Figure 9	Numerical model trials designed to investigate horizontal heterogeneities within the well skin.....	39
Figure 10	Normalized head versus time plots of the horizontal heterogeneity trials.....	40
Figure 11	Numerical model trials designed to investigate radial heterogeneities within the well skin.....	41
Figure 12	Normalized head versus time plots of the radial heterogeneity trials.....	42
Figure 13	Normalized head versus time plots of the skin thickness trials.	43
Figure 14	Normalized head versus time plots of the various partial penetration and screen location trials in a thin aquifer	45
Figure 15	Normalized head versus time plots of the various partial penetration and screen location trials in a thick aquifer.	46

LIST OF FIGURES CONTINUED

<u>FIGURE</u>		<u>PAGE</u>
Figure 16	Normalized head versus time plots of the anisotropy trials	48
Figure 17	Conceptual model showing the cylinder design of DPPS	50
Figure 18	Conceptual model showing the layering design of DPPS	52
Figure 19	DPPS spreadsheet interface for data entry	53
Figure 20	Validation of DPPS to the Theis analytical model	56

CHAPTER 1

INTRODUCTION

The success of any groundwater investigation hinges largely on an accurate determination of hydraulic conductivity (K). Numerous studies (Sudicky, 1986; Zhang and Neuman, 1990; Butler et al., 1996; 1999) have shown that K impacts everything from contaminant transport to remediation system design. The most widely used methods involve either large-scale multiple pumping well tests or small-scale single well tests, also called slug tests. Current research has concentrated on alternative methods involving direct-push (DP) methods that do not rely on the installation and development of traditional monitoring wells. While all of these methods have their advantages and drawbacks, their general acceptance has led to the development of analytical solutions to solve the governing equations for a wide variety of conditions. These analytical solutions have built-in assumptions that often limit their effectiveness in heterogeneous, real-world environments.

The continued acceptance and application of existing analytical models centers on their simplicity and reliability. Most of the numerical models built to overcome the limitations of the analytical solutions either were created in the infancy of computer technology or are so complicated to be impractical for the practicing professional. The purpose of this dissertation was to develop numerical modeling codes designed specifically for hydrologic tests that can handle complex groundwater systems yet still be relatively simple to apply. The new code was also used to investigate the impact of complex well skins on the recovery of single well tests.

BACKGROUND

Large-scale multiple well pumping tests, which withdraw water at a constant rate and measure subsequent aquifer head response in the test well and surrounding observation wells, have historically yielded aquifer properties. The problem associated with these tests is the large manpower, equipment, and monetary commitment required for completion. Small-scale single well tests offer an alternative approach. These tests, also called slug tests, yield a response in a well to an instantaneous change in water level. While slug tests do have potential drawbacks, such as scale issues or inaccurate response because of insufficient well development; their use has become common over the last couple of decades. Slug tests have minimal equipment requirements, can be completed in fairly short periods of time, and are relatively easy to perform (Butler, 1998).

Recently, research has investigated alternatives to single and multiple well tests. Cho et al. (2000), Butler et al. (2002), and McCall et al. (2002) have all explored direct-push (DP) technology to determine K . DP technology refers to the process of driving, pushing, or vibrating small-diameter hollow steel rods into unconsolidated sediments, usually to depths less than 30 meters. DP technology can complete tasks that traditional drilling methods such as hollow stem auger or mud rotary have performed including the collection of soil and groundwater samples and the installation of permanent monitoring wells. The advantages of DP include lower associated costs, faster drilling time, generation of minimal waste, and less smearing of lower permeability materials on the borehole wall which can lead to the underestimation of hydraulic conductivity (USEPA, 1997). These advantages have led to the development of single well testing

methodologies used in the small diameter rods of direct push drill rigs (Butler et al., 2002).

The success of single well testing applied to DP wells hinges on the removal of fine material around the screen during development. In order to overcome this limitation, the Kansas Geological Survey (KGS) developed a method, termed the Direct Push Permeameter (DPP), which is relatively insensitive to the disturbed zone created by the advancement of the direct push rods. The DPP utilizes a specialized tool that consists of two pressure transducers positioned above a short screened interval. While the small-diameter probe is advanced into the subsurface, water is injected at a constant rate, usually less than 300 milliliters per minute, to keep the screen clear of debris. Pushing and water injection cease once the desired depth of the test is reached. Before the actual test is performed, pressure heads are allowed to recover to background conditions. The test is then performed by injecting water through the screen at a constant rate and monitoring the resultant pressure variations at the two transducer locations. DPP has the potential to improve the vertical spatial resolution of K, which has always been an issue in contaminant transport studies (Taylor et al., 1990; Melville et al., 1991). Hydraulic conductivity can be obtained on a much finer-scale, perhaps even as fine as every few inches. This method can also provide storage properties, which usually cannot be accurately obtained through single well tests.

OBJECTIVES

This dissertation has three objectives. The first objective is the development and validation of a numerical groundwater modeling code with the capabilities of simulating

slug tests with a high degree of accuracy. While there are existing cylindrical numerical models, many of them were designed in the late 1970s and early 1980s when computer technology was still in its infancy. These early models required the use of supercomputers that may have taken days to converge for a single model in complex groundwater systems. However, the exponential growth in computing power in the last decade has made complex cylindrical finite-difference models much more accessible than older numerical models. Today, desktop and laptop computers have reached incredible speeds and model simulations, even in heterogeneous conditions, only take mere minutes to converge. Numerical models developed more recently such as RADFLOW (Johnson et al., 2001) still have limitations such as coarse cylinder spacing directly adjacent to the well and coarse time steps, which may affect the accuracy of the model. The numerical modeling code developed for this research, termed Slug Test Simulator (STS), is designed to be flexible enough to handle complex conditions, fast enough to be practical, and is simple enough to be easily integrated into field projects.

The second objective involves a detailed investigation of the well skin influence on aquifer head response. A well skin refers to the presence of a disturbed zone around a well produced by drilling or pushing activities in association with the installation of a monitoring well (Henebry and Robbins, 2000). In most cases, auger rotation can smear clay and silt-sized particles on the borehole wall, creating an artificial barrier to groundwater flow (Yang and Gates, 1997). This skin effect can be responsible for decreased flow over time as finer-grained particles are transported to the well screen where they are trapped, creating blockages (Butler, 1998). Unfortunately, the success of slug tests largely hinges on the removal of this fine-grained material surrounding the well

screen during development activities. Numerous studies have investigated the impact of a well skin on a slug test with analytical models. However, these models are limited to specific boundary conditions. In contrast, numerical models can simulate the impacts of a well skin under conditions too complex for analytical models. STS will be used to study the influence of certain skin properties such as specific storage, skin thickness, anisotropy, and partial penetration on head responses.

The last objective involves the development and validation of another numerical modeling code designed to simulate DPP tests. Due to the specialized nature of these tests, their accuracy can not be compared to any existing analytical or numerical model. The spherical form of Darcy's Law (equation 1) is only valid for steady-state flow; not the transient flow conditions created by DPP tests. Existing numerical models such as RADFLOW (Johnson et al., 2001) incorporate such a coarse cylinder spacing that the small head changes induced by these tests could not be predicted with any great accuracy. Therefore, STS was modified to produce the Direct-Push Permeameter Simulator (DPPS). DPPS is similar to STS with its ability to handle well skins, partial penetration, and layered heterogeneities. The numerical code also has a flexible spreadsheet interface and displays the head at the two pressure transducer locations.

PREVIOUS WORK

Analytical Studies

Early studies in hydrology attempted to determine how drawdown from a pumping well could yield hydraulic conductivity and storage parameters. The first mathematical solution for analyzing transient drawdown data from constant, multiple

well tests in confined aquifers was published by Theis (1935; 1940). With some underlying assumptions, Theis arrived at a nonequilibrium equation to determine both transmissivity and storage properties. The petroleum engineers van Everdingen and Hurst (1949) applied the material balance equation describing the flow of fluids with low compressibility in porous media to wells with both water and oil present. They developed type curves for constant discharge tests with the assumption that the pumping well can be approximated as a line sink with no skin effects. Hantush and Jacob (1954) and Hantush (1956) revised the Theis solution to include the situation where leakage from an overlying aquitard contributes water to the well. Neuman (1975) incorporated gravity drainage in anisotropic unconfined aquifers to produce theoretical type curves for the analysis of multiple well test data. Newer work by Butler (1990) investigated the role of multiple well tests in site characterization and found that under anisotropic conditions, the effects of near-well properties can introduce considerable error into conductivity measurements. In order to reduce these errors, the observation wells in these studies should be placed at greater distances away from the pumping well.

Groundwater flow in the vicinity of a pumping well can be influenced by the presence of a low permeability well skin. Early advances were made in the petroleum engineering field involving the analysis of fluid flow in the presence of a fine-grained well skin (Hurst, 1953; van Everdingen, 1953). Novakowski (1989) presented a composite analytical solution and generated type curves to explore the effects of wellbore storage and a heterogeneous conductivity skin on head distribution. Cassiani et al. (1999) designed a semi-analytical solution for partially penetrating wells in a confined aquifer that accounted for wellbore storage, infinitesimal skin, and anisotropy. Chen and Chang

(2003) developed a two-dimensional curve-matching model to investigate the response of constant discharge tests in unconfined aquifers with skin effects. Chiu et al. (2007) developed a mathematical model for pumping tests on partially penetrating wells with radial heterogeneous aquifer properties.

With the advent of single well tests, analytical research began to focus on the mathematical problem of how to convert aquifer head response from a slug test to determine hydraulic conductivity. Hvorslev (1951) observed that the total flow or volume of water required for the equalization of hydrostatic pressure in a piezometer was directly related to the permeability of the soil. He was one of the first to develop a systematic method to calculate soil permeability from slug test data, although he noted that errors within the methodology often produce low values not indicative of the porous media. Later, Ferris and Knowles (1954) showed that an aquifer's transmissivity could be estimated from the slope of a plot of the hydraulic head versus the reciprocal of time if the well is modeled as a line source with an infinitesimal diameter. Cooper et al. (1967) presented a series of semi-log type curves to calculate the transmissivity and storage coefficients of confined aquifers from tests completed on wells with finite radii. Cooper and others also showed that Ferris and Knowles' line source solution is a good approximation to the finite well case when time since the start of the test is sufficiently large. Papadopoulos et al. (1973) developed additional type curves for the Cooper et al. (1967) methodology useful for low permeability aquifers. Bouwer and Rice (1976) introduced a method for the analysis of unconfined single well test data based on the steady-state Thiem (1906) equation and experiments with electrical analog models. Newer methods such as the KGS semi-analytical model (Hyder et al., 1994) can

overcome most of the limitations of the classical solutions; but still cannot match the flexibility of numerical models.

While slug tests have become the standard field technique to determine K , research has aimed to quantify the impact of well skins on slug test accuracy. Ramey et al. (1975) introduced semi-log and log-log curves that included the effects of both wellbore storage and skin effects. Faust and Mercer (1984) and Moench and Hsieh (1985) discovered that the hydraulic conductivity of the well skin creates a distinct shift of CBP type curves to the right, leading to inaccurate values of aquifer conductivity. Numerous field studies (McElwee et al., 1990; Hyder and Butler, 1995; Yang and Gates, 1997; Butler and Healey, 1998) have investigated the effects of well skin and have concluded that it remains the main reason why hydraulic conductivity is often underestimated in slug tests. In fact, Hyder and Butler (1995) assessed the effect of a low permeability well skin and determined that the error can be as high as 30% with the estimate of K more representative of the skin conductivity. Henebry and Robbins (2000) conducted field experiments to determine hydraulic conductivity in multilevel samplers before, during, and after development and found that post-development K values were 3.2 to 9.6 times higher than pre-development values.

While traditional single and multiple well tests have historically been the standard to determine aquifer properties, they are often very limited in scope, can produce substantial inaccuracies due to their strong dependence on well characteristics, and incorporate data analysis procedures that have very limiting assumptions (Butler, 1998). Also, the K derived from these well tests represents an average over the entire screened interval. Butler et al. (1994) and McCall et al. (2002) have discovered that K can vary

substantially in the vertical direction. Taylor et al. (1990) evaluated some of the older methods to determine the vertical distribution of hydraulic conductivity such as straddle packer tests, grain-size analysis, and single well electrical tracer tests. They concluded that all methods have significant drawbacks including vertical leakage in straddle packer tests, the fact that grain-size analyses don't incorporate the influence of micro-scale structure and packing, and the need for injection of large volumes of fluid in an electrical tracer test. The limitations of these traditional methods have resulted in the development of new methodologies including multilevel slug tests and dipole flow tests.

Multilevel slug tests can distinguish vertical variations in K often needed to accurately describe plume movement in contaminant transport. This method is an extension of the traditional single well test in which a portion of the screen is isolated by packers to determine K at several vertical locations within the screened interval.

Traditional analysis techniques such as Cooper et al. (1967), Bouwer and Rice (1976), and Dagan (1978) are not adequate for multilevel slug tests since these methods assume that vertical flow is negligible. Hayashi et al. (1987) developed one of the first analytical solutions for multilevel slug tests in isotropic confined systems. Widdowson et al. (1990) later presented a general solution used to predict K over a wide range of geometries and flow conditions. Melville et al. (1991) compared the results of multilevel slug tests with tracer tests performed on a confined aquifer in Alabama and found relatively good agreement between the two methods. Zlotnik and McGuire (1998) expanded the Springer-Gelhar (1991) model to handle oscillatory responses of multilevel slug tests in high- K formations.

Another current method, the dipole flow test (DFT), involves recirculatory flow to estimate aquifer properties. Initially, packers are inflated to isolate two intervals, or chambers, of the well screen. During the test, water is continuously pumped at a constant rate creating circulatory flow between the aquifer and the two chambers. Kabala (1993) was the first to develop solutions for DFT applications by extending Hantush's (1961a) analytical solution to determine chamber drawdown in these recirculation wells under confined or leaky confined conditions for a homogenous aquifer. Zlotnik and Ledder (1996) developed new DFT solutions for the case involving an aquifer of infinite thickness and explored the effects of boundary conditions on dipole tests. Hvilshoj et al. (2000) tested the Kabala (1993) analytical method and concluded that the reliability of the K estimates based solely on the pressure head data were questionable and added that more precise results required the use of an inverse numerical multilayer flow model. Zlotnik et al. (2001) approached the analysis of dipole tests from a new perspective looking at drawdown within each chamber instead of looking at the head differences between chambers. They found that most DFTs generally reach equilibrium quickly and are not influenced greatly by the presence of aquifer boundaries or anisotropy.

The major limitation of the current generation of aquifer testing is that most of these methods can only be used in traditional monitoring wells, which may be screened across a relatively large portion of the aquifer and may involve the presence of low permeability skins. Although multilevel slug tests and dipole tests can provide detailed vertical K distributions, the presence of fine-grained material around the well screen can substantially influence the K estimate. Direct Push (DP) technology can eliminate many of these problems. In addition, DP offers greater mobility, simplicity, no generation of

hazardous waste material, less site disturbance, simplicity, and low cost (Butler et al., 2002).

Hinsby et al. (1992) were the first to attempt single well tests in small one-inch DP drive points. They developed a drive-point methodology to determine the vertical distribution of hydraulic conductivity and applied different analytical models to test the accuracy of their model. By matching their model to results obtained through two natural gradient tracer tests conducted at the site, they concluded that their methodology provided a reasonable estimate of local K. Bjerg et al. (1992) used that same method to perform over 330 single well tests at a field site in an unconfined sandy aquifer and found that the results from the slug tests corresponded well to tracer test results done in the same area. Cho et al. (2000) and McCall et al. (2002) separately developed both equipment and procedures for measuring vertical K profiles using DP methods. McCall et al. (2002) tested their field methods and found that their results differed by 3-12% compared to results obtained from multilevel slug tests. Butler et al. (2002) performed perhaps the most comprehensive investigation and concluded that K estimates from DP methods are essentially indistinguishable from those done in conventional wells.

Research has focused on one particular DP test, the DPP, due to its ability to overcome limitations associated with a disturbed zone around the screen. DPP tests utilize pumping-induced head gradients between two transducers. Hydraulic conductivity is calculated based on the steady-state spherical form of Darcy's Law (Butler et al., 2007):

$$K_r = \frac{Q_r \left(\frac{1}{r_1} - \frac{1}{r_2} \right)}{4\pi(\Delta h)} \quad (1)$$

where K_r is the radial hydraulic conductivity; Q_r is the radial volumetric flow rate (length³/time); r_1 and r_2 are the distances from the center of the screen to the pressure transducers. Equation 1 can be derived by simply applying the surface area of a sphere to Darcy's Law as shown in equation 2.

$$Q_r = K_r (4\pi r^2) \frac{dh}{dr} \quad (2)$$

Separation of the terms yields:

$$Q_r \int_{r_1}^{r_2} \frac{dr}{r^2} = 4\pi K_r \int_{h_1}^{h_2} dh \quad (3)$$

To solve the left hand side of the equation, the general power formula is used:

$$\int u^n du = \frac{u^{n+1}}{n+1} \quad \therefore \int u^{-2} du = \frac{u^{-1}}{-1} = -\frac{1}{u} \quad (4)$$

Integration yields equation 5, which simplifies to equation 1.

$$Q_r \left[-\frac{1}{r_2} + \frac{1}{r_1} \right] = 4\pi K_r (h_2 - h_1) \quad (5)$$

Numerical Studies

Most early research concentrated on the development of analytical solutions for single and multiple well tests. Numerical models; however, are superior in that they can handle complex real-world conditions and are not restricted by many of the assumptions associated with analytical models. Rushton and Booth (1976) developed the first two-zone numerical model that could handle both layering effects and variations in aquifer parameters of multiple well test data. They realized that most analytical solutions were inadequate to analyze pumping test behavior in heterogeneous environments and advocated the use of numerical models instead. Rushton and Chan (1976) used the same

numerical model to simulate conditions when hydraulic conductivity and storage parameters vary with depth and obtained reliable results for confined, leaky, and unconfined situations. Rathod and Rushton (1984) originally designed a one-dimensional numerical model based on the lumped parameter solution of the governing equation that was later adapted to include flow in both the radial and vertical directions (Rathod and Rushton, 1991). Rutledge (1991) created an axisymmetric model to handle well casing storage, head loss across the well screen, and head losses due to frictional forces. Johnson et al. (2001) created RADFLOW, a Fortran-based cylindrical finite-difference model that interfaces with Microsoft Excel, to analyze multiple well test data.

Most current numerical solutions (Rathod and Rushton, 1991; Reilly and Harbaugh, 1993; Johnson et al., 2001) were designed for pump tests; not for the mechanics of slug tests. However, there have been a few studies using numerical models to investigate aquifer response from slug tests. Demir and Narasimhan (1994) applied the TRUST numerical model, a finite-element algorithm used for saturated-unsaturated flow in deformable porous media, to evaluate the accuracy of the Hvorslev method. Further research by Brown et al. (1995) involved another comparison of the TRUST model to the Bouwer-Rice method (1976). They discovered that while the Bouwer and Rice method was superior to Hvorslev, it still tended to underestimate K. Recently, Bohling and Butler (2001) developed a radial, two-dimensional, finite-difference model (lr2dinv) primarily to determine vertical K variations for multilevel slug tests.

CHAPTER 2

SLUG TEST SIMULATOR (STS)

DERIVATION OF GOVERNING EQUATION

The governing equation was derived using the lumped parameter approach for radial flow as first presented by Rushton and Redshaw (1979). Rathod and Rushton (1991) used this same lumped parameter approach in their derivation of the governing equation for the specific case when an overlying aquifer contributes leakage to a lower confined aquifer. Our model incorporates a block-centered approach and includes assumptions of layered heterogeneity and anisotropic conditions. The model does allow for heterogeneous conditions in the radial direction in order to simulate the effects of a variable conductivity well skin. However, the model assumes homogeneous radial hydraulic conductivity in the formation. Cylindrical finite-difference modeling uses the radial form of Darcy's Law as shown in equation 6.

$$Q_r = K_r 2\pi r b \frac{dh}{dr} \quad (6)$$

where b is the layer thickness. Separation of the terms yields:

$$Q_r \int_{r_1}^{r_2} \frac{dr}{r} = 2\pi K_r b \int_{h_1}^{h_2} dh \quad (7)$$

where h_1 and h_2 are the hydraulic heads in two adjacent cylinders; r_1 and r_2 are the radii from the center of the well to the center of the respective cylinders where h_1 and h_2 are measured. Equation 6 assumes that the pumping rate (Q_r) at any given time can be considered a constant and brought outside the integral. For radial flow, this is not exactly true, but reasonable over short spatial intervals. Integration of equation 7 yields:

$$Q_r (\ln r_2 - \ln r_1) = 2\pi K_r b (h_2 - h_1) \quad (8)$$

A new term (a) will represent the logarithmic cylinder spacing as originally presented by Ruston and Redshaw (1979) where:

$$a = \ln r_2 - \ln r_1 = \ln \frac{r_2}{r_1} \quad (9)$$

Substitution and rearrangement yields:

$$Q_r = \frac{2\pi K_r b (h_2 - h_1)}{a} \quad (10)$$

Flow from an outer cylinder into a center cylinder, denoted Q_{oc} , and flow from a center cylinder into an inner cylinder (Q_{ci}) can be written as equations 11 and 12.

$$Q_{oc} = \frac{2\pi K_r b (h_o - h_c)}{a} \quad (11)$$

$$Q_{ci} = \frac{2\pi K_r b (h_c - h_i)}{a} \quad (12)$$

where h_i , h_c and h_o are the hydraulic heads in the inner, center, and outer cylinders, respectively (see figure 1). In a two-dimensional case, the model needs to account for vertical flow from an upper cylinder into the center cylinder (Q_{uc}) and flow from the center cylinder into a lower cylinder (Q_{cl}) as shown below.

$$Q_{uc} = \frac{\pi K_z (r_c^2 - r_i^2) (h_u - h_c)}{(z_u - z_c)} \quad (13)$$

$$Q_{cl} = \frac{\pi K_z (r_c^2 - r_i^2) (h_c - h_l)}{(z_c - z_l)} \quad (14)$$

where $\pi(r_c^2 - r_i^2)$ represents the cross-sectional area of vertical flow; h_l and h_u are the heads in the lower and upper cylinders; K_z is the vertical hydraulic conductivity; z_u , z_c , and z_l

are the elevations that correspond to the center of the cylinders where the hydraulic heads h_u , h_c , and h_l are measured (figure 1).

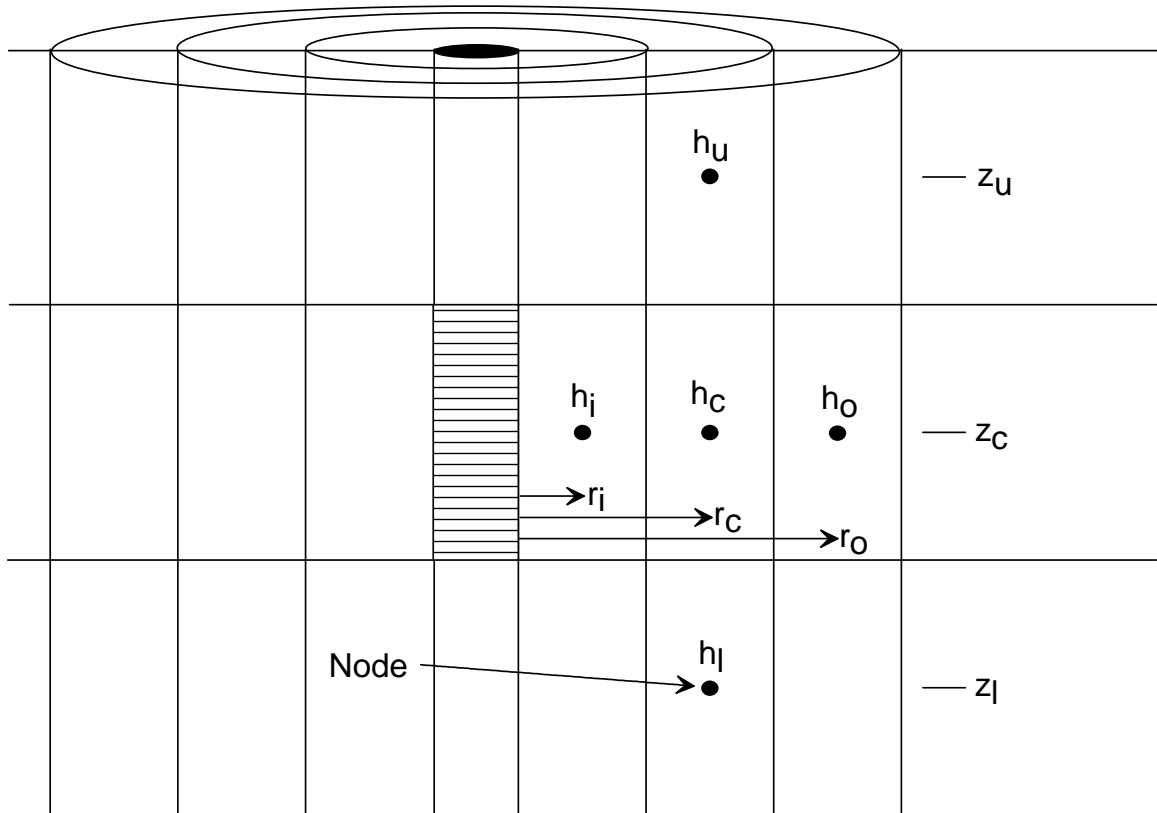


Figure 1: Cross-sectional view of a hypothetical aquifer used for the derivation (notation explained in text)

Using the principle of conservation of mass, flow into the center cylinder is a function of the flow from the inner and outer cylinders in the radial direction and flow from the upper and lower cylinders in the vertical direction, which is equal to the change in storage as shown in equation 15.

$$Q_{ic} + Q_{oc} + Q_{uc} + Q_{cl} = S_f S_A \frac{\Delta h}{\Delta t} + R \quad (15)$$

where S_f is the storage factor (dimensionless); S_A is the surface area of the center cylinder (length^2); $\Delta h/\Delta t$ is the change in head per time; and R represents all external sources of flow ($\text{length}^3/\text{time}$). The storage factor represents either elastic storativity (S) under confined conditions or gravity drainage from specific yield (S_y) for unconfined flow. The numerical model requires specific storage (S_s) (length^{-1}) to be input by the user and converts it to a dimensionless parameter by multiplying by the saturated thickness of the cylinder.

The center cylinder has a doughnut shape in plan view. Its cross-sectional area is the distance from the edge of the center cylinder to the edge of the inner cylinder squared multiplied by pi. However, the cylinder edges are unknown. Therefore, the cross-sectional area was calculated by using the distances to the nodes of the cylinders as shown in equation 16.

$$S_A = (\pi r_c^2) - (\pi r_i^2) = \pi(r_c^2 - r_i^2) \quad (16)$$

where r_c and r_i are the radii from the center of the well to the middle of the center and inner cylinders, respectively. Although this is not the actual cross-sectional surface area, the error is small as long as the cylinder sizes remain small. Additional experiments with various methods to calculate cross-sectional area including one used by Rushton and Redshaw (1979) yielded approximately the same answer.

To determine the change in head with respect to time, a backward finite-difference approximation is used where $\Delta h/\Delta t$ becomes:

$$\frac{\Delta h}{\Delta t} = \frac{h_c^m - h_c^{m-1}}{t_m - t_{m-1}} \quad (17)$$

where h_c^m is the new head in the center cylinder at current time; h_c^{m-1} is the old head in the center cylinder at the previous time; t_{m-1} and t_m are the previous and current times, respectively.

All variables independent of the hydraulic heads are grouped into conductance terms.

$$C_i = C_o = \frac{2\pi K_r b}{a} \quad (18)$$

$$C_u = \frac{\pi K_z (r_c^2 - r_i^2)}{(z_u - z_c)} \quad (19)$$

$$C_l = \frac{\pi K_z (r_c^2 - r_i^2)}{(z_c - z_l)} \quad (20)$$

Everything on the right hand side of the equation not involving heads is grouped into a constant term:

$$w = \frac{S_f \pi (r_c^2 - r_i^2)}{(t_m - t_{m-1})} \quad (21)$$

Substitution of equations 18, 19, 20, and 21 into equation 15 produces:

$$C_i h_i + C_o h_o + C_u h_u + C_l h_d - (w + C_i + C_o + C_u + C_l) h_c^m = -w h_c^{m-1} + R \quad (22)$$

All conductance and constant terms are grouped together into a new term (E):

$$E = w + C_i + C_o + C_u + C_l \quad (23)$$

Substituting equation 23 into equation 22 and solving for head in the center cylinder yields equation 24.

$$h_c^m = \frac{(C_i h_i + C_o h_o + C_u h_u + C_l h_d + w h_c^{m-1} - R)}{E} \quad (24)$$

The question arises whether the hydraulic heads of the adjacent cylinders (inner, outer, upper, and lower) in equation 24 are calculated at the beginning of the time step (m-1) or

the end of the time step (m). For a fully implicit version, the space derivative is assumed to be best approximated at the end of the time step (m) while the fully explicit version has the best approximation at the beginning of the time step (m-1). In practice, the spatial heads in the adjacent cells may be calculated as a weighted average of the heads at both t_m and t_{m-1} . The weight (α) lies somewhere between 0 and 1. In this system, a fully explicit version would have a weight of $\alpha=0$ while a fully implicit version would have $\alpha=1$. The general form is shown in equation 25.

$$\text{WeightedAverage} = (\alpha * h_c^m) + ((1 - \alpha) * h_c^{m-1}) \quad (25)$$

The Crank-Nicolson method assumes that the best approximation lies somewhere between the implicit and explicit forms and therefore uses an α of 0.5 (Wang and Anderson, 1982). The explicit method involves a direct solution of the governing mathematical equations while implicit forms must solve a system of equations with multiple unknowns. Implicit models are iterative in nature where an initial “guess” is allowed to slowly converge towards the correct solution. For this method, an average head for the inner, outer, and lower cylinders are calculated in the following manner:

$$h_c^a = (0.5 * h_c^m) + (0.5 * h_c^{m-1}) \quad (26)$$

where h_c^a is the Crank-Nicolson average head in the center cylinder. Once the Crank-Nicolson solution is applied, hydraulic head in the center cylinder is calculated through equation 27, which is the governing equation of the numerical modeling codes.

$$h_c^a = \frac{(C_i h_i^a + C_o h_o^a + C_u h_u^a + C_d h_d^a + w h_c^{m-1} - R)}{E} \quad (27)$$

The Gauss Seidel iterative procedure solves the system of equations, calculating a new hydraulic head value based on a function of the head in the surrounding four cylinders

(inner, outer, upper, and lower). This methodology essentially sweeps through the grid and calculates the resultant head from two known head values at the beginning of the time step (h^{m-1}) and two unknown head values at the end of the time step (h^m):

$$h_{i,j}^{m+1} = \frac{h_{i-1,j}^{m+1} + h_{i,j-1}^{m+1} + h_{i+1,j}^m + h_{i,j+1}^m}{4} \quad (28)$$

where i represents the vertical layers and j represents the radial cylinders. The program then replaces h^{m-1} with h^m after each calculation and thus relaxes the residuals, or differences between the two values, making it more efficient and faster than other methods (Wang and Anderson, 1982). The Visual Basic code for STS is presented in appendix A.

CYLINDRICAL FINITE-DIFFERENCE MODELING CODE

STS simulates two-dimensional, axial symmetric flow to a well induced by an instantaneous change in head. The numerical model consists of concentrically stacked cylinders centered on a well where the first cylinder is directly adjacent to the screen (figure 2). STS was built to handle a variety of conditions including unconfined flow, partial penetration, presence of a variable conductivity well skin, and layered heterogeneities. The model incorporates small time steps and cylinder spacing to improve model accuracy.

Cylinder Spacing

Two different approaches were taken to model the cylinders for the well skin and the cylinders for the formation. The cylinders directly adjacent to the screen that simulate the well skin have a constant spacing which is calculated based on the total width of the skin and the number of skin cylinders to be modeled, both of which are user

defined. The formation cylinders utilize a logarithmic expansion, which is dependent on an initial radius, as shown in equations 29 through 31.

$$\text{InitialRadius} = \text{WellRadius} + \text{SkinRadius} \quad (29)$$

$$G = \text{Log}(\text{InitialRadius}) - \text{Log}(\text{WellRadius}) \quad (30)$$

$$\text{Radius}(j) = \text{Radius}(j-1) \times G \quad (31)$$

where $\text{Radius}(j)$ and $\text{Radius}(j-1)$ are the center cylinder and inner cylinders respectively.

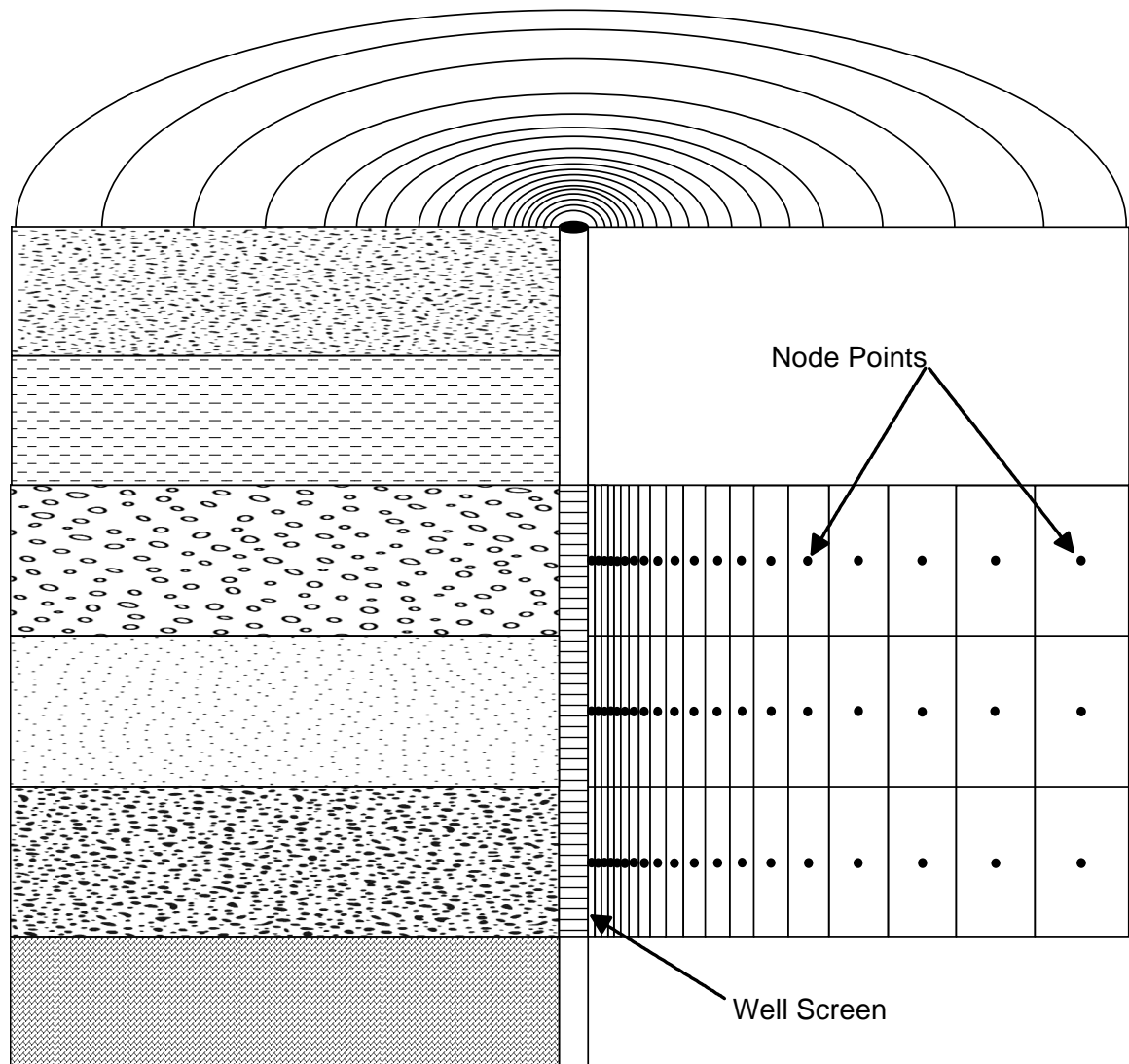


Figure 2: Conceptual model showing the design of STS

The width of the last cylinder in the well skin is used to calculate the first cylinder radius in the formation. If the user chooses not to model a well skin, an arbitrary well skin radius comprised of one cylinder with a width of 0.01 meters (1 cm) is set with the same properties as the formation. This was necessary to set up the logarithmic expansion of the cylinders that occurs adjacent to the last skin cylinder. The number of cylinders defined by the user must be large enough so that head changes in the outer cylinders are negligible.

Well Skin

One of the key features of this model is its ability to incorporate the presence of a well skin adjacent to the screen. This skin can represent a highly porous sand pack or a lower permeability well skin often created over time as finer-grained particles are transported to the well screen. There are a few existing analytical and numerical models that can handle the presence of homogeneous well skin adjacent to the screened interval such as the KGS semi-analytical model (Hyder et al., 1994) and the KGS numerical model, lr2dinv (Bohling and Butler, 2001). STS extends on these earlier models by simulating a heterogeneous, anisotropic skin. In order to accomplish this, modified conductivity arrays were established in both the radial (KRT) and vertical (KZT) directions as shown in equations 32 and 33.

$$KRT(i, j) = \frac{2\pi K_r}{\text{Log}(\text{Radius}(j)) - \text{Log}(\text{Radius}(j-1))} \quad (32)$$

$$KZT(i, j) = 2 * \text{Area}(j) * K_z \quad (33)$$

where Area(j) is the plan view cross-sectional area. A heterogeneous skin may produce conditions where K in adjacent cylinders is distinctly different. In this case, the harmonic

mean was utilized to calculate the conductance in the radial direction in the skin and the vertical direction as shown in equations 34 and 35.

$$C_r = \frac{2 * KRT(i, j) * KRT(i, j + 1)}{KRT(i, j) * KRT(i, j + 1)} * Thickness(i, j) \quad (34)$$

$$C_v = \frac{\frac{2 * KZT(i, j) * KZT(i + 1, j)}{KZT(i, j) + KZT(i + 1, j)}}{Thickness(i + 1, j) + Thickness(i, j)} \quad (35)$$

where $KRT(i, j)$ and $KRT(i, j + 1)$ are the modified radial conductivity arrays for the center and outer cylinders; $KZT(i, j)$ and $KZT(i + 1, j)$ are the modified vertical conductivity arrays for the center and upper cylinders; and $Thickness(i, j)$ and $Thickness(i + 1, j)$ are the vertical thicknesses of the center and upper cylinders, respectively. The impact of a heterogeneous skin on the analysis of slug tests will be explored in Chapter 3.

Boundary Conditions

For our model, the outer boundary was placed at a sufficient distance away from the well using the logarithmic spacing discussed above to produce negligible changes in hydraulic head at the boundary. The inner boundary at the well screen is simulated as a specified head boundary, which changes with each time step. Head in the well is explicitly calculated by adding the total discharge in each of the cells adjacent to the screen and subtracting the volumetric flow within the well itself for each time step:

$$WellHead = WellHead - \frac{WellFlow * Time}{\pi * WellRadius^2} \quad (36)$$

The test continues until the well reaches a user-defined recovery.

Specified flux or Neumann boundary conditions are applied to both the lower and upper boundaries. A no-flow boundary is automatically assigned to the bottom of the

lowermost cylinder, representing the bottom of the flow system. The upper boundary is determined by specifying the flux across the water table, or the amount of recharge added to the system. STS uses a rewetting feature similar to that found in MODFLOW (McDonald and Harbaugh, 1988) to handle unconfined conditions where wet cells can be deactivated or dry cells rewetted in the presence of a falling or rising water table. STS compares the elevation of the water table in relation to the bottom elevation of a particular cylinder (figure 3). In the case of a falling water table (figure 3a), if the water table falls below the bottom elevation of the upper cylinder, the upper cylinder status is set to zero and that cylinder is turned off. The hydraulic head of the lower cylinder is set to zero and that cylinder is turned off. The hydraulic head of the lower cylinder is set to the elevation of the water table. In the presence of a rising water table (figure 3b), if the head rises above the bottom elevation of a cylinder, STS turns the cylinder back on and sets its status as active. At the same time, STS sets the head of the upper cylinder to the water table elevation and the head of the lower cylinder to the bottom elevation of the

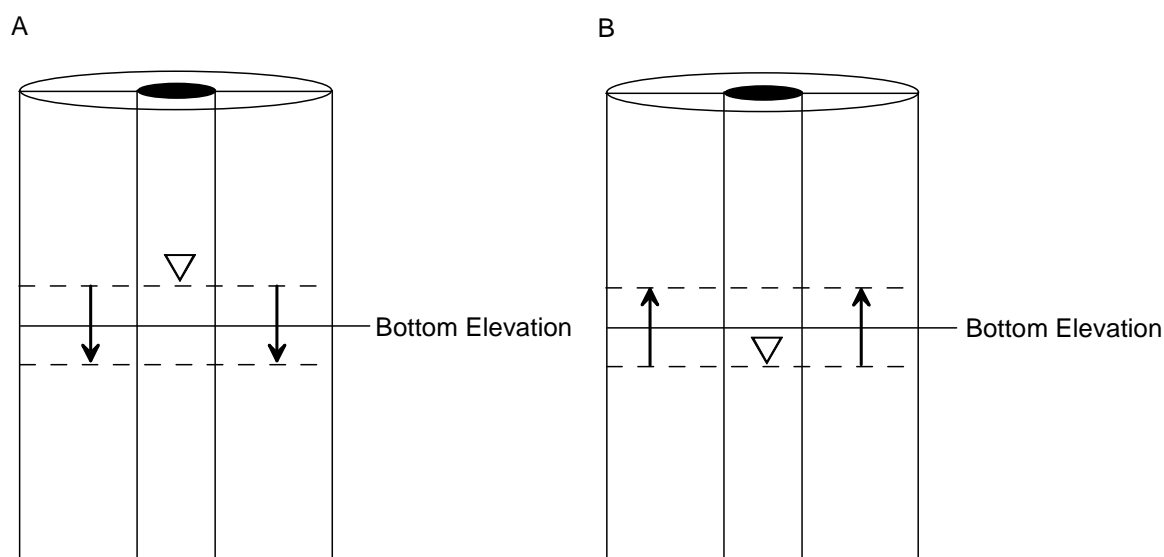


Figure 3: Diagram of the rewetting feature used in STS to handle both falling and rising water tables under unconfined conditions

upper cylinder. If a cell contains the water table, the storage term is set to specific yield; otherwise the storage term is set to specific storage.

User Interface

STS was developed with a spreadsheet interface in which users input well geometry, skin and formation properties, model variables, and hydraulic head into a simple template (figure 4). The geometry of the formation with respect to the well screen must be known including the depth to the screen, screen length, and total saturated

SLUG TEST SIMULATOR

Geometry

0.0254	Well casing radius
0.0254	Well screen radius
175	Number of cylinders

Run STS

Flow System

Confined
 Unconfined

Model Status

10.010094	Wellhead
100.0	% Completion

Formation Properties

Homogeneous Formation Properties

10	Formation thickness
0.0001	Radial hydraulic conductivity
0.0001	Vertical hydraulic conductivity
6.60E-04	Specific storage (confined case)
1.00E-02	Specific yield (unconfined case)

Screen Characteristics

4	Depth from top of formation to top of the screen
2	Length of the well screen
2	Number of model layers above the screen
1	Number of model layers within the screen
2	Number of model layers below the screen

Hydraulic Head

10	Initial head in well
1	Maximum displacement

Skin Properties

Well skin present around screen

0.0354	Well skin radius
10	Number of skin cylinders
6.60E-03	Specific storage of the skin (confined case)
1.00E-02	Specific yield of the skin (unconfined case)

Homogeneous skin conductivity

0.00001	Radial skin hydraulic conductivity
0.00001	Vertical skin hydraulic conductivity

Model Variables

1.00E-08	Initial time
0.00001	Tolerance
0.01	Recovery
0.5	Alpha

Figure 4: STS spreadsheet interface for data entry

thickness. Certain model variables are hard-wired into the code and set to values that produce optimal results. These variables include those that control grid discretization (see cylinder spacing section above) and time discretization. The initial time step, which is originally set at 1e-8 seconds for all STS trials, can be changed by the user. However,

any value below this produces conditions when the model has trouble converging to a solution and any value above this may adversely affect the accuracy of the model. STS calculates subsequent time steps based on the head differences between the head in the well and the head in the first cylinder. If the difference is greater than $4e-6$ units, time is calculated based on equation 37; if the difference is less than $4e-6$ units, time is based on equation 38.

$$Time = Time / 1.005 \quad (37)$$

$$Time = Time * 1.005 \quad (38)$$

STS allows users to choose between homogeneous or heterogeneous properties for both the well skin and formation. Model input allows the user to set a homogenous K for the skin or manually input hydraulic conductivity for the well skin in the radial and vertical directions in a separate Conductivity spreadsheet. In the case of a homogeneous formation, STS divides the model into equal layers, dependent on the user-defined number of layers above, within, and below the screen and their respective thicknesses. On the other hand, if the user chooses a heterogeneous formation, properties such as layer thickness, storage, and hydraulic conductivity are entered in a separate Layer Property spreadsheet. For a heterogeneous simulation with multiple conductivity values, STS automatically selects the radial conductivity in the first screen layer in order to calculate dimensionless time. While properties can vary between layers, they must be modeled as homogeneous within each layer. This assumption is reasonable since most aquifer properties, especially hydraulic conductivity, often vary more between layers as opposed to within layers in the radial direction.

The duration of the simulation depends on several factors including whether the formation is homogenous or heterogeneous, the formation storage, the presence of a well skin, the total number of cylinders, and recovery. Homogenous formations with no skin and large storage values usually converge within ten to fifteen minutes, while heterogeneous formations with variable conductivity skins and low storage values ($<10^{-5}$) may take an hour or more to run.

Model output is displayed in several worksheets. Final heads, the dimensionless parameters, and radii of all the cylinders are printed to the Well Results worksheet along with a graphical plot of dimensionless head versus dimensionless time. The Well Results sheet also contains the model's budget, expressed as a percent error, which depends on the volumetric flow out of the well and the volumetric flow within all of the model's cylinders (equation 39).

$$PercentError = \frac{(CellFlow - WellFlow)}{(WellFlow)} \times 100 \quad (39)$$

In a layered model, the final heads for all layers are displayed in the Aquifer Heads spreadsheet. In most cases, hydraulic conductivity of the formation is unknown, but the user can compare their field data to a plot of normalized head versus time from the model in the Field Analysis spreadsheet. Through a trial-and-error process, the user can match the curves to determine the hydraulic conductivity of the tested unit.

Comparison of Model Features

The capabilities of STS can be better illustrated through a head-to-head comparison with another numerical slug testing code; lr2dinv (Bohling and Butler, 2001). STS and lr2dinv are both cylindrical two-dimensional finite-difference models developed to simulate slug tests that can incorporate partial penetration, anisotropy, and well skins.

However, the programs have distinct differences. Lr2dinv is a fully implicit model ($\alpha=1$) while STS allows the user to set alpha anywhere from a fully explicit model ($\alpha=0$) to a fully implicit model ($\alpha=1$). STS trials for this study utilized the Crank-Nicolson method, which assumes that the best approximation lies somewhere between the two end members with $\alpha=0.5$.

Lr2dinv is a FORTRAN-based program with a rigid input structure that writes the resultant hydraulic heads to a text file with no ability to graphically display the results. STS, on the other hand, has a spreadsheet-based interface that allows for more flexibility. STS allows the user to systematically change parameter values on the data entry sheet while automatically plotting the dimensionless time versus dimensionless head recovery curves. STS also has a field analysis spreadsheet that allows the user to compare field data from slug tests to the numerical model's recovery curves. The model's parameters can be varied through a trial-and-error process to determine the hydraulic conductivity of the field site.

Lr2dinv cannot simulate unconfined aquifers. The KGS designed Lr2dinv for confined conditions with a zero flux upper boundary; making it impossible to model partially saturated cells during simulations. STS, on the other hand, can handle unconfined conditions by tracking a cell's status, which allows saturated cells to dewater as the water table falls and dry cells to rewet as the water table rises. The numerical model uses specific storage if a cell is completely saturated, but switches to specific yield if the cell is only partially saturated. Butler (1998) suggested that models do not need to address specific yield since specific storage has a greater impact on slug tests. However, in high permeability aquifers with the water table position within the screened interval,

this might not be entirely true. In any case, the ability of STS to include both specific storage and specific yield may produce more accurate results for unconfined aquifers.

Both codes were built to handle the mechanics of slug tests, but different approaches led to minor discrepancies in the model's conceptual design. The most important of these distinctions is how both models handle the inner boundary at the well. The KGS placed the first cylinder inside of the well in *lr2dinv* to handle the effects of wellbore storage and the placement of packers in the well. STS creates the first cylinder outside of the well. *lr2dinv* requires the user to define both the time and grid discretization while STS has these features built into the code to produce optimal results. In order to simulate a well skin in *lr2dinv*, the grid expansion must be designed so that the cylinder radii fall on top of the nodes, which in many cases is awkward. STS treats the well skin cylinders independently from the formation cylinders. STS has a constant spacing for the well skin cylinders, which is created through user-defined skin thickness and the number of skin cylinders. The cylinders simulating the formation utilize a logarithmic spacing as discussed in the derivation section. In *lr2dinv*, the layer spacing is fixed, but layer spacing above, below, and within the screened interval can be set separately in STS.

MODEL VALIDATION

Validation of a numerical code essentially demonstrates its accuracy by comparing the numerical solution to those of well established analytical models. The Cooper-Bredehoeft-Papadopoulos (CBP) (1967) analytical method and the Kansas

Geological Survey (Hyder et al., 1994) semi-analytical solution were chosen for comparison purposes.

The CBP (1967) produces semi-log type curves to interpret slug test data for a fully penetrating well in a confined aquifer. Model trials were designed to simulate the CBP solution in which normalized head was plotted against the Tt/r_c^2 term (where T is transmissivity; t is time; and r_c is the well casing radius) originally developed by CBP for an aquifer with storativity (α) values of 10^{-1} , 10^{-3} , and 10^{-5} . The data from the numerical model coincide with the analytical curves (figure 5).

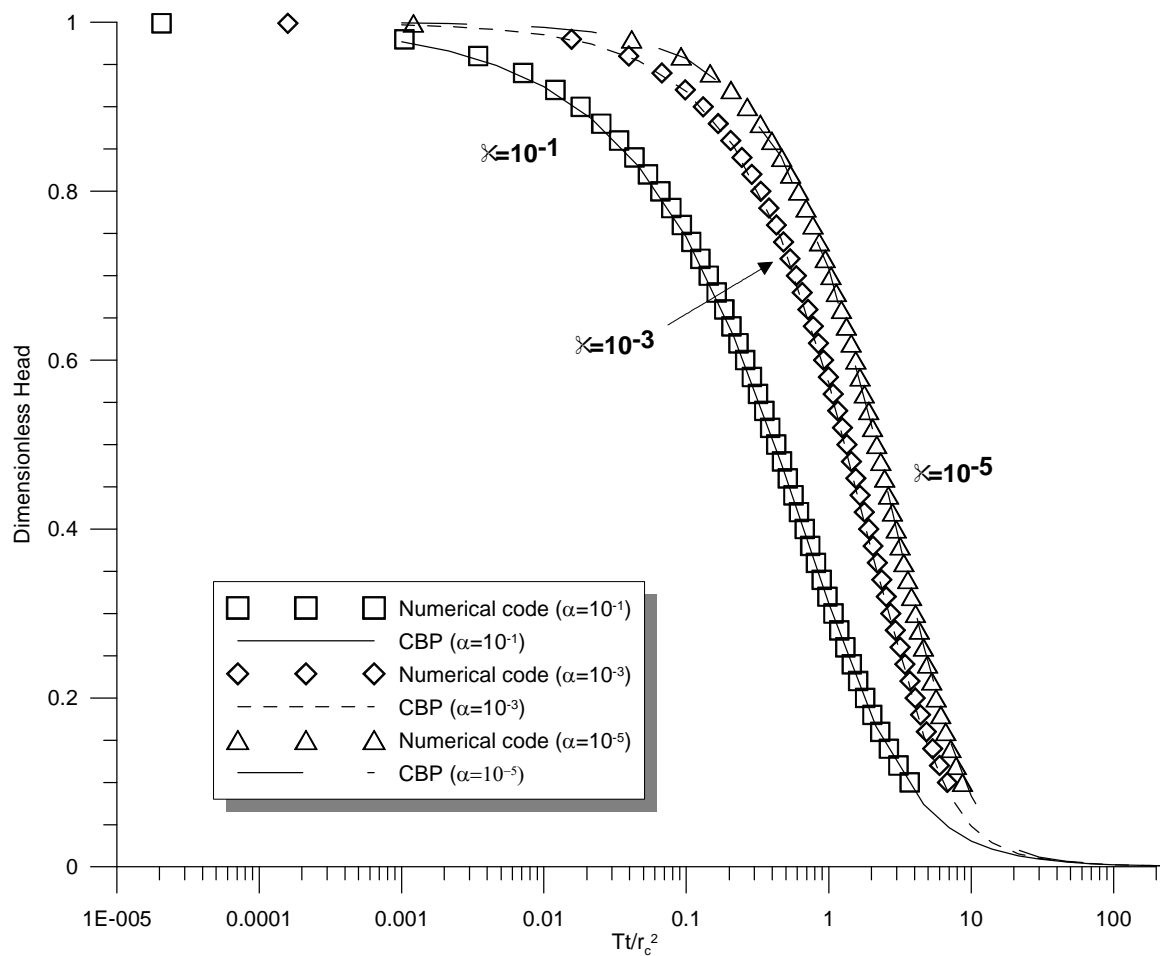


Figure 5: Normalized head versus time plots of STS compared to the CBP analytical model

The KGS extends the CBP (1967) method to handle partially penetrating wells with a vertical flow component and the presence of a well skin. The KGS solution, originally presented by Hyder et al. (1994), utilizes a plot of normalized head versus the logarithm of dimensionless time to generate a series of type curves with each curve representing a particular storage value (Butler, 1998). Since the importance of our numerical model lies in its ability to handle partial penetration and well skin effects, a match to the KGS solution was crucial. Therefore, STS was compared to the KGS model in four individual cases to see if it could reproduce a wide array of conditions (table 1).

Table 1: Parameter values used in the comparison of STS to the KGS analytical solution

	<i>Case 1</i> <i>No skin</i>	<i>Case 2</i> <i>Lower K Skin</i>	<i>Case 3</i> <i>Unconfined</i>	<i>Case 4</i> <i>Anisotropy</i>
<i>Well radius</i>	0.0254 m	0.0254 m	0.0508 m	0.0254 m
<i>Formation b</i>	10 m	10 m	20 m	5 m
<i>Depth from top of formation to top of screen</i>	4 m	4 m	8 m	2 m
<i>Screen length</i>	2 m	2 m	4 m	1 m
<i>Well skin radius</i>	--	0.0354 m	--	0.0454 m
K_r (skin)	--	0.000001 m/s	--	0.00001 m/s
K_z (skin)	--	0.000001 m/s	--	0.000001 m/s
S_s (skin)	--	0.032 m ⁻¹	--	0.05 m ⁻¹
K_r (formation)	0.0001 m/s	0.0001 m/s	0.0001 m/s	0.0001 m/s
K_z (formation)	0.0001 m/s	0.0001 m/s	0.000001 m/s	0.00001 m/s
S_s (formation)	0.0014 m ⁻¹	0.0014 m ⁻¹	0.003 m ⁻¹	0.002 m ⁻¹
<i>Condition</i>	Confined	Confined	Unconfined	Confined

In all four cases, the numerical model results are extremely similar to the KGS semi-analytical curves (figure 6).

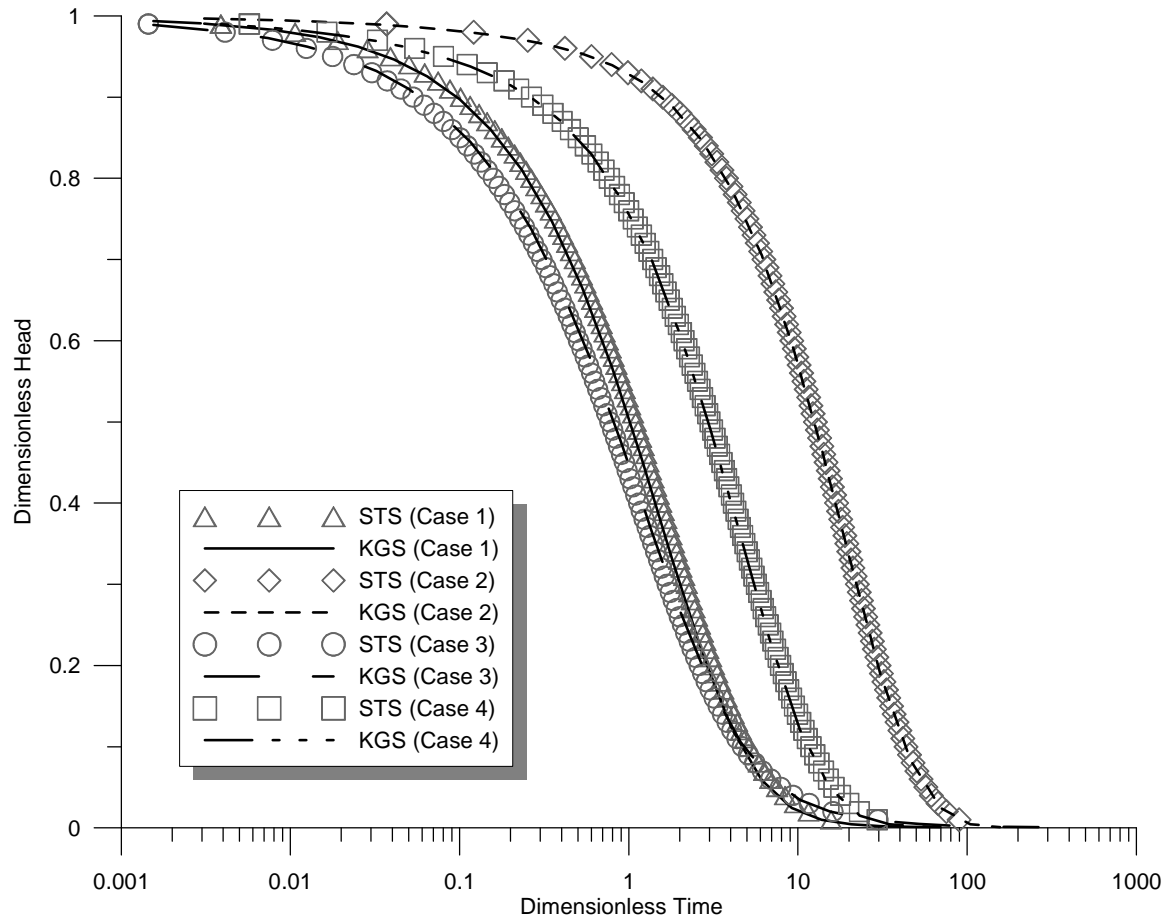


Figure 6: Normalized head versus time plots of STS compared to the KGS semi-analytical model

A comparison between the KGS semi-analytical model and STS does indicate some differences in the model results. Through model trials, it was determined that any S_s greater than $1e-4 \text{ m}^{-1}$ produced results where the curves from KGS and STS were identical. However, small deviations between the curves were apparent with any lower storage values. Second, the KGS treats the water table as an infinite source or sink while STS allows the water table to move up or down, depending on the conditions present.

While this distinction is relatively trivial, it does produce cases where the resultant curves are not identical.

CHAPTER 3

WELL SKIN

NUMERICAL MODEL TRIALS

STS was designed to simulate two-dimensional radial flow to a well after an instantaneous change in hydraulic head from a slug test. The mathematical foundation, capabilities, and validation of the STS numerical modeling code are discussed in greater detail in Chapter 2. One of the key features of STS is its ability to simulate heterogeneous, anisotropic well skins. The presence of a lower permeability well skin has been shown to influence the aquifer response induced by the slug test, producing K values not representative of the geologic materials. Conductivity estimates may also be impacted by the presence of a high permeability sand pack in tight formations, creating two distinct head response curves. An important part of this research was to measure the impact of a well skin on the resultant head responses. Therefore, trials were designed to determine the overall response of the model to changes in skin properties such as specific storage, hydraulic conductivity, anisotropy, partial penetration, thickness, and the position of the well screen.

Most model trials described in this paper were developed for a test case. Model runs simulated a confined aquifer consisting of 5 layers; 2 layers above and below the well screen with one layer representing the screened interval. The well screen has a radius of 0.0254 meters, a length of 2 meters, and is perfectly centered within the aquifer (symmetric conditions). The formation beyond the skin has a saturated thickness of 10 meters, the same radial and vertical hydraulic conductivity of 0.0001 meters per second

(m/s), and has a specific storage of $6.6e-4 \text{ m}^{-1}$. The well skin is 0.01 meters thick, has radial and vertical hydraulic conductivity one order of magnitude lower than that of the aquifer (0.00001 m/s), and a specific storage of $6.6e-3 \text{ m}^{-1}$. The initial hydraulic head in the formation and well is 10 meters and the maximum displacement during the falling head slug test is 1 meter.

Specific Storage

Like the CBP (1967) analytical and the KGS (Hyder et al., 1994) semi-analytical models, STS is highly dependent on the specific storage of the geologic materials. Model trials show that specific storage is the primary controlling factor of the location of the recovery curves of normalized time versus normalized head. Ranges for specific storage used in the trials were obtained from Walton (1988) and Cheng (2000) and are summarized in Table 2.

Table 2: Specific Storage values used in model simulations

GEOLOGIC MATERIAL	SPECIFIC STORAGE (S_s) (M^{-1})	AVERAGE S_s USED IN MODEL TRIALS (M^{-1})
Clay	$3.2e-3 - 3.2e-2$	$6.6e-3$
Sand/Sand and Gravel	$2.6e-4 - 2.6e-3$	$6.6e-4$

While most model trials incorporate the average specific storage values shown in table 2, initial trials were set up to determine the effect of the two specific storage end members. Clay was simulated with the highest specific storage shown above ($3.2e-2 \text{ m}^{-1}$) and a representative low hydraulic conductivity of $1e-9 \text{ m/s}$ (Fetter, 2001) while the sand and gravel end member contained the lowest specific storage ($2.6e-4 \text{ m}^{-1}$) and a representative high hydraulic conductivity of 0.01 m/s (Fetter, 2001). Figure 7 shows a significant

offset between the two curves, indicating that specific storage coupled with changes in hydraulic conductivity can strongly influence the results.

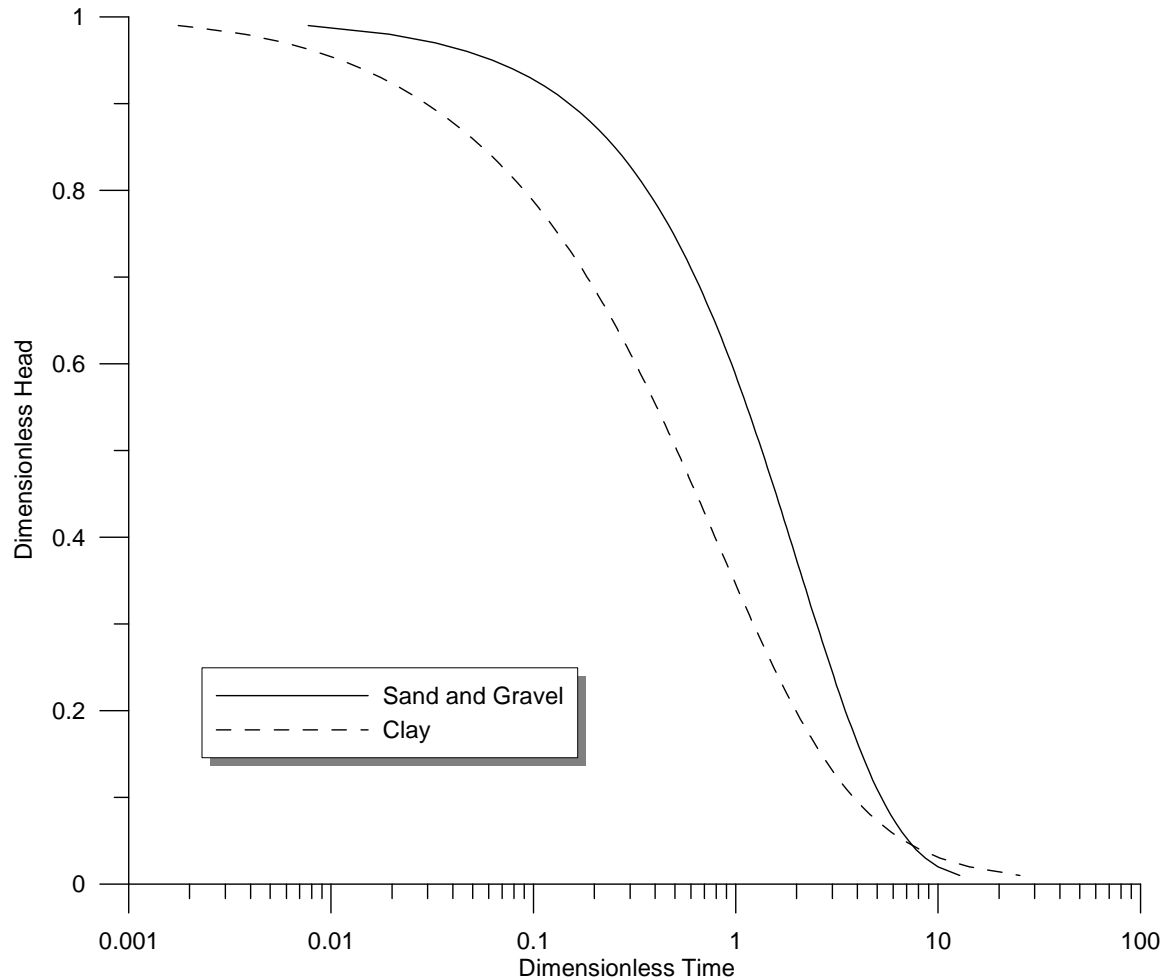


Figure 7: Normalized head versus time plots generated by the two specific storage end members

Well Skin Characteristics

Well skins are zones around the borehole that exhibit different hydraulic properties than that of the geologic formation. These skins can be composed of lower permeability materials, often called positive skins (Yang and Gates, 1997), which are created through well installation procedures or over time as fine-grained particles are

mobilized toward the screen. On the other hand, negative skins may exist in low permeability formations if the sand pack has a higher conductivity than that of the surrounding media. Figure 8 shows a plot of normalized head versus time for the no skin case, the positive skin case (skin K is one order of magnitude lower than formation), and the negative skin case (skin K is one order of magnitude greater than formation). While both types of skins will influence groundwater flow near the screen, these trials suggest that positive skins have a much greater impact on hydraulic head response.

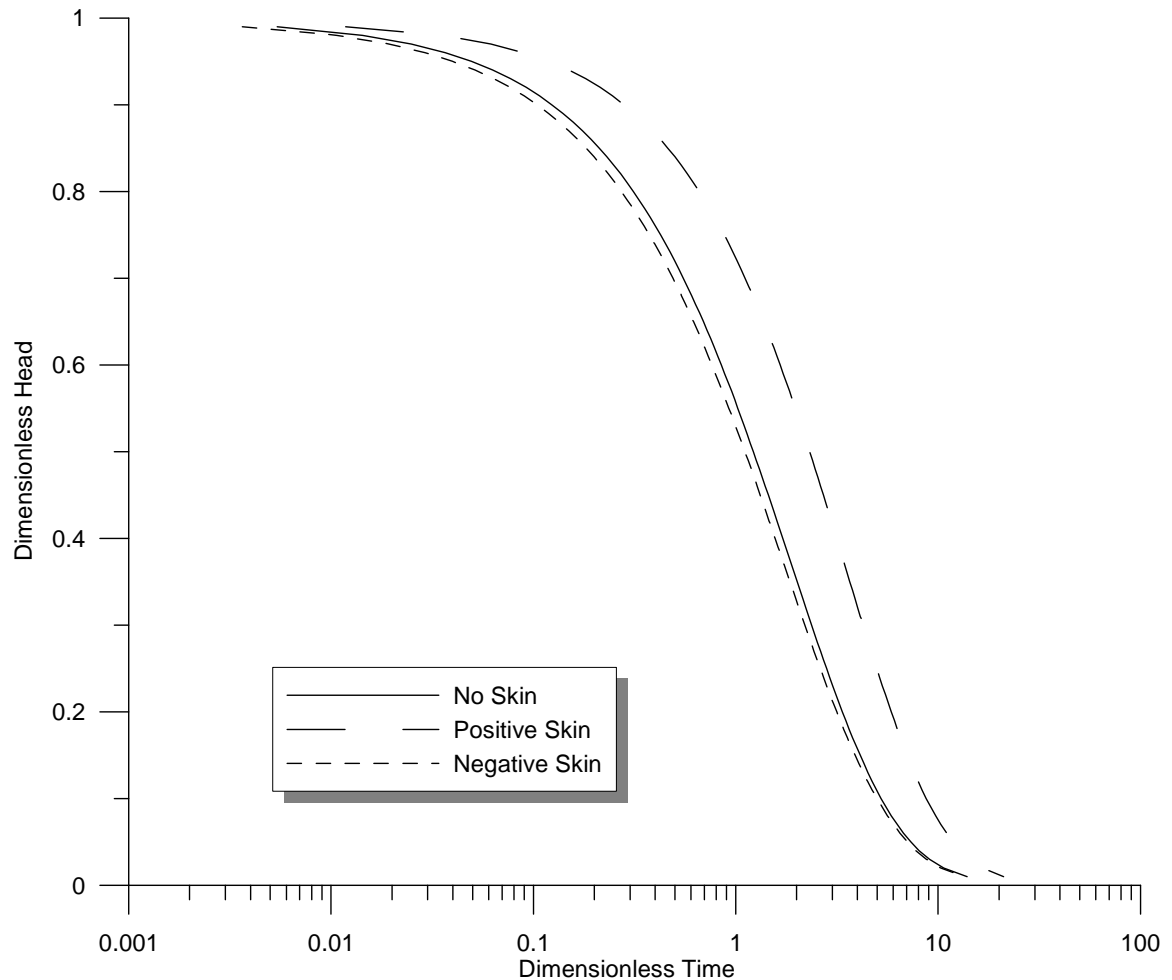


Figure 8: Normalized head versus time plots showing the effects of both positive and negative well skins

While development activities such as pumping or bailing may clean out a portion of the screened interval, a skin may remain over portions of the screen or adjacent to the well casing above and below the screen. Therefore, the well skin may vary dramatically vertically and away from the borehole. In order to simulate this, STS allows the user to vary the hydraulic conductivity within the skin both in the vertical and horizontal directions. In this case, the numerical model reads the radial hydraulic conductivity from a worksheet and calculates the horizontal and vertical hydraulic conductivities using the harmonic mean between two adjacent cylinders.

Figure 9 shows the design of the various trials used to quantify the impact of layered horizontal heterogeneities within the skin while figure 10 shows the resultant normalized head versus time plots. If the screened interval is completely free of a skin and modeled with the same hydraulic conductivity as the formation, the curve generated is similar to the no skin case, regardless of the K distribution of the skin above and below the screen. Trials 1 and 3 display this pattern as they both start off slightly underneath the no skin case, but as time goes on, all three curves merge. This indicates that early in the test, the lower permeability sections above and beneath the skin are playing a minor role in influencing the test. However, as time goes on, most of the radial flow is being concentrated in the higher K conduit next to the screen and flow in the lower permeability sections is negligible. On the other hand, if the screened interval has a conductivity one order of magnitude lower than the formation and one order of magnitude higher than the surrounding skin, then the recovery curve is identical to the homogeneous skin case as shown by trials 2 and 4. In this case, radial flow in the higher permeability screened interval overwhelms flow in the sections above and below the

screen. This causes the skin to act as if it is homogeneous in nature even though there are distinct layers with different conductivities.

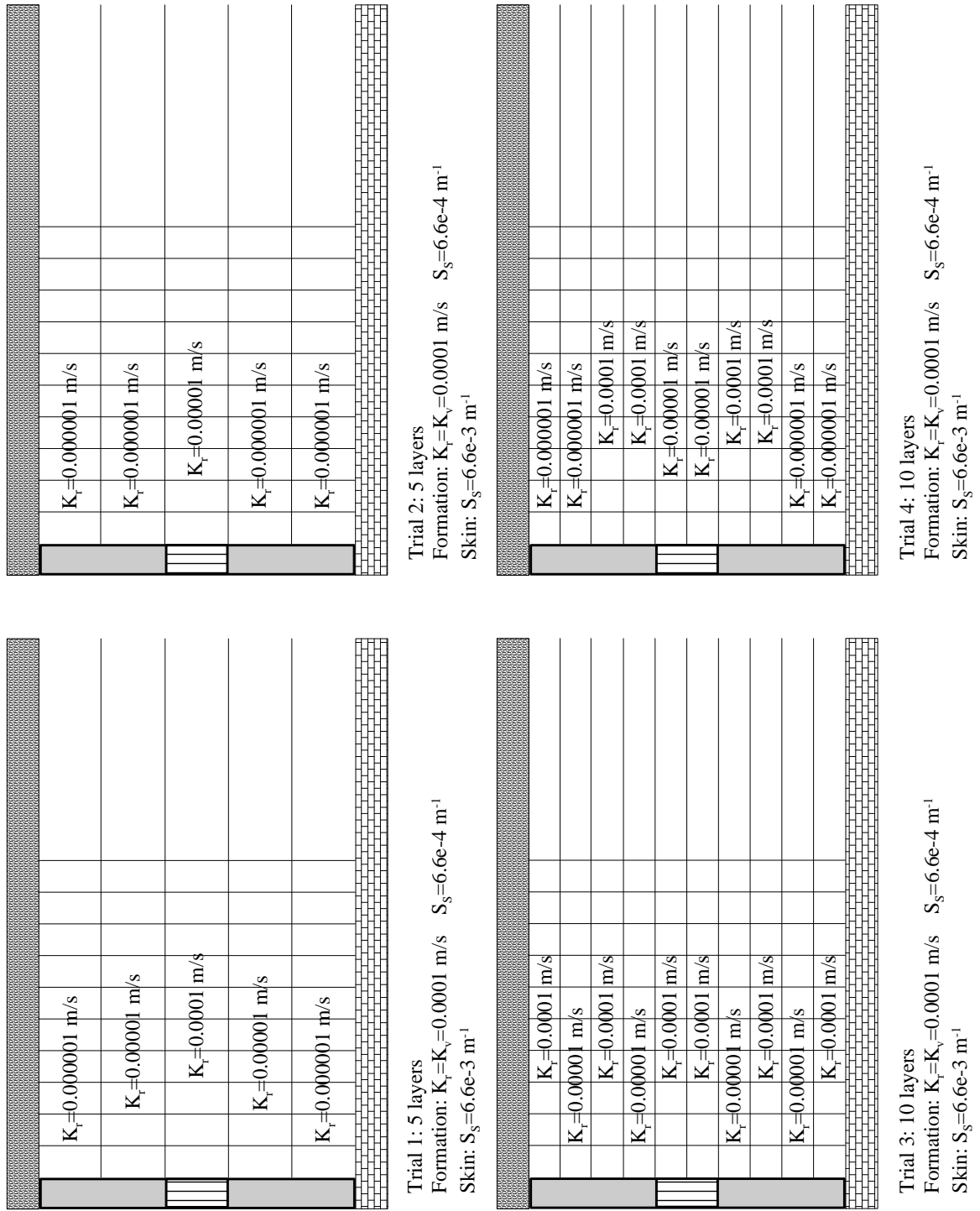


Figure 9: Numerical model trials designed to investigate horizontal heterogeneities within the well skin

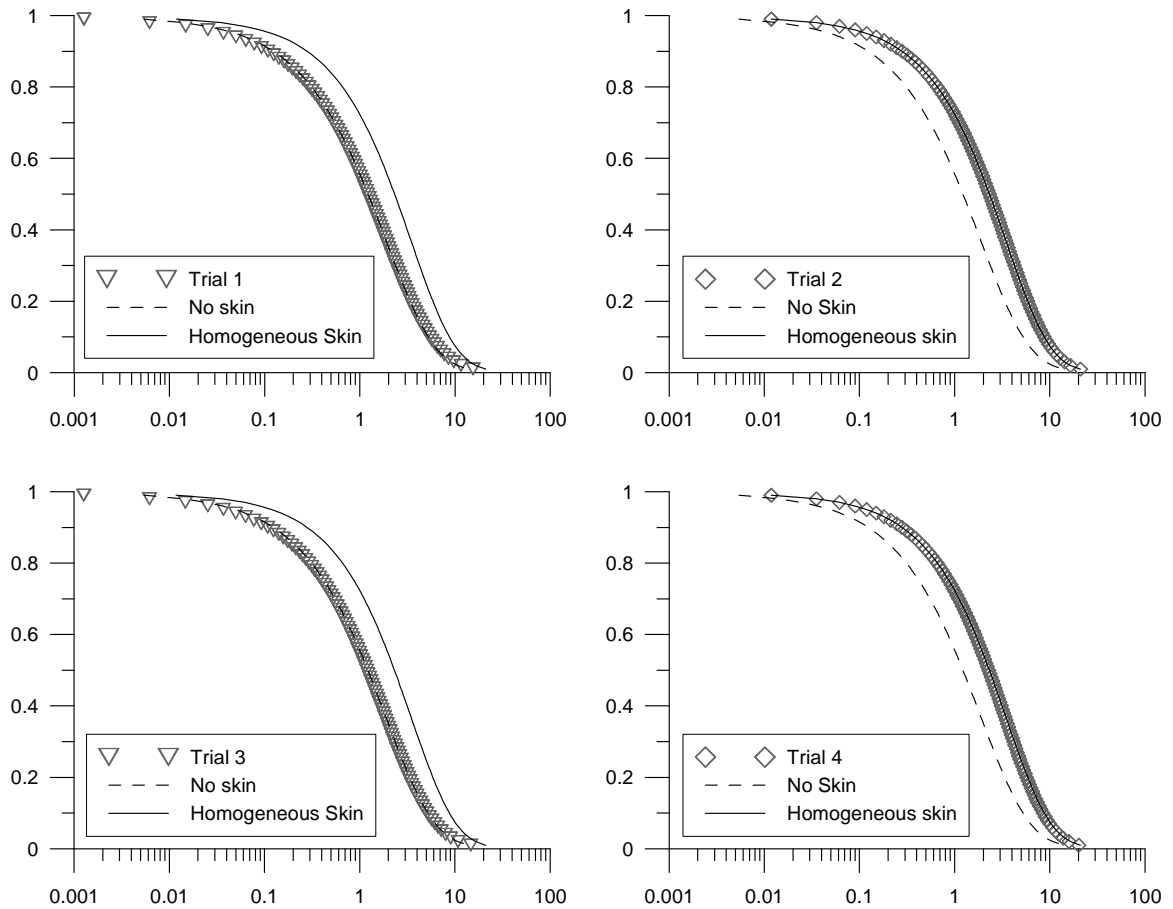


Figure 10: Normalized head versus time plots of the horizontal heterogeneity trials. Trials 1 and 3 have skin layers within the screen with the same K as the formation while trials 2 and 4 have layers with K one order of magnitude lower than the formation.

Further simulations explored the impact of radial heterogeneity in the skin.

Figure 11 shows the design of the various trials with the resultant curves displayed in figure 12. The first two trials involved 4 distinct zones spanning the entire formation thickness with the skin conductivity progressively increasing (trial 5) or decreasing (trial 6) in a linear manner away from the screened interval. It is important to note that the conductivity zones within the skin are still less permeable than the formation itself. In both cases, the recovery curves are shifted dramatically to the right when compared with the homogeneous skin case (figure 12), suggesting that the individual zones are acting as

barriers to delay head response from the slug test. The remaining two trials involved varying the skin K in both the radial and vertical directions, creating six distinct zones

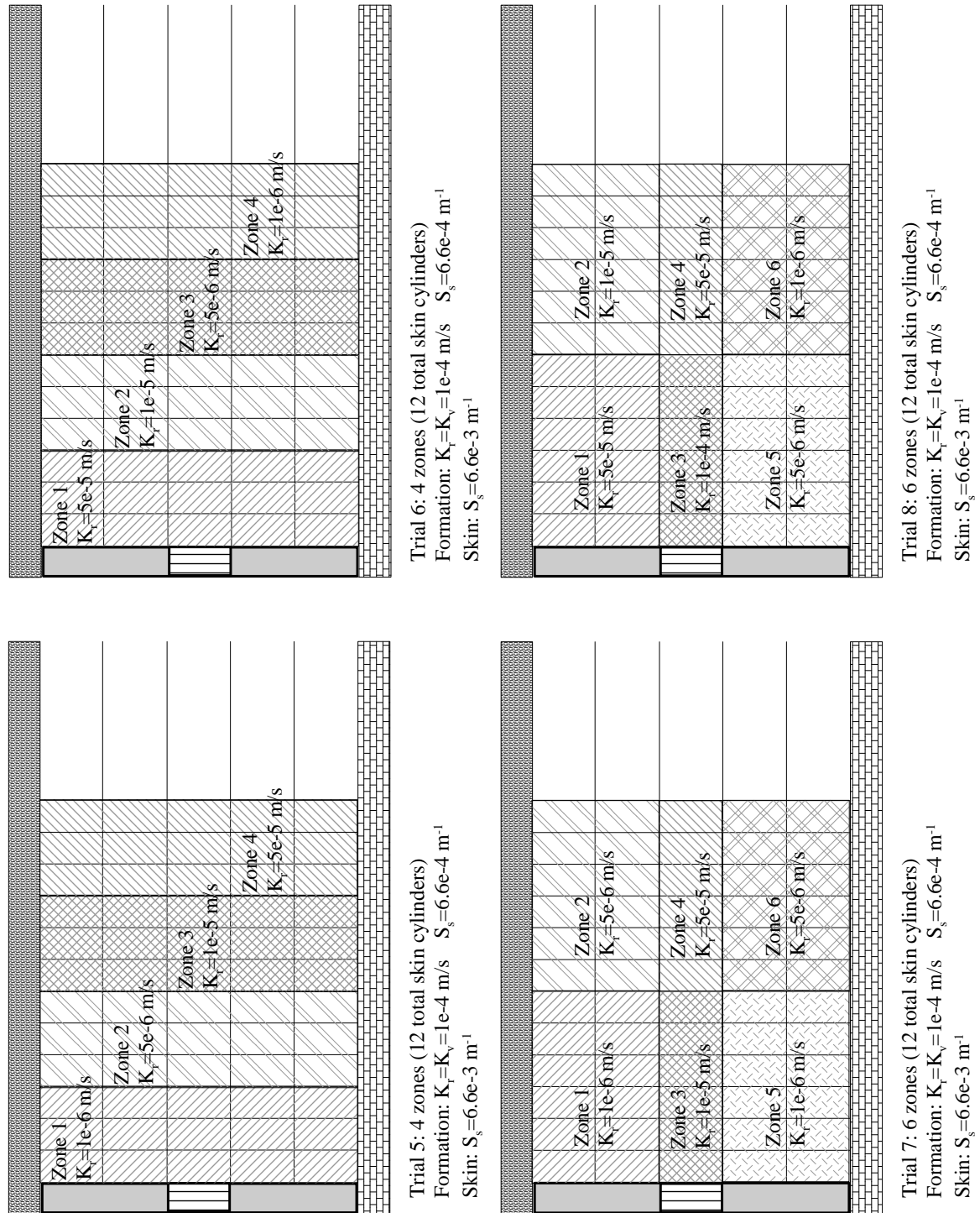


Figure 11: Numerical model trials designed to investigate radial heterogeneities within the well skin

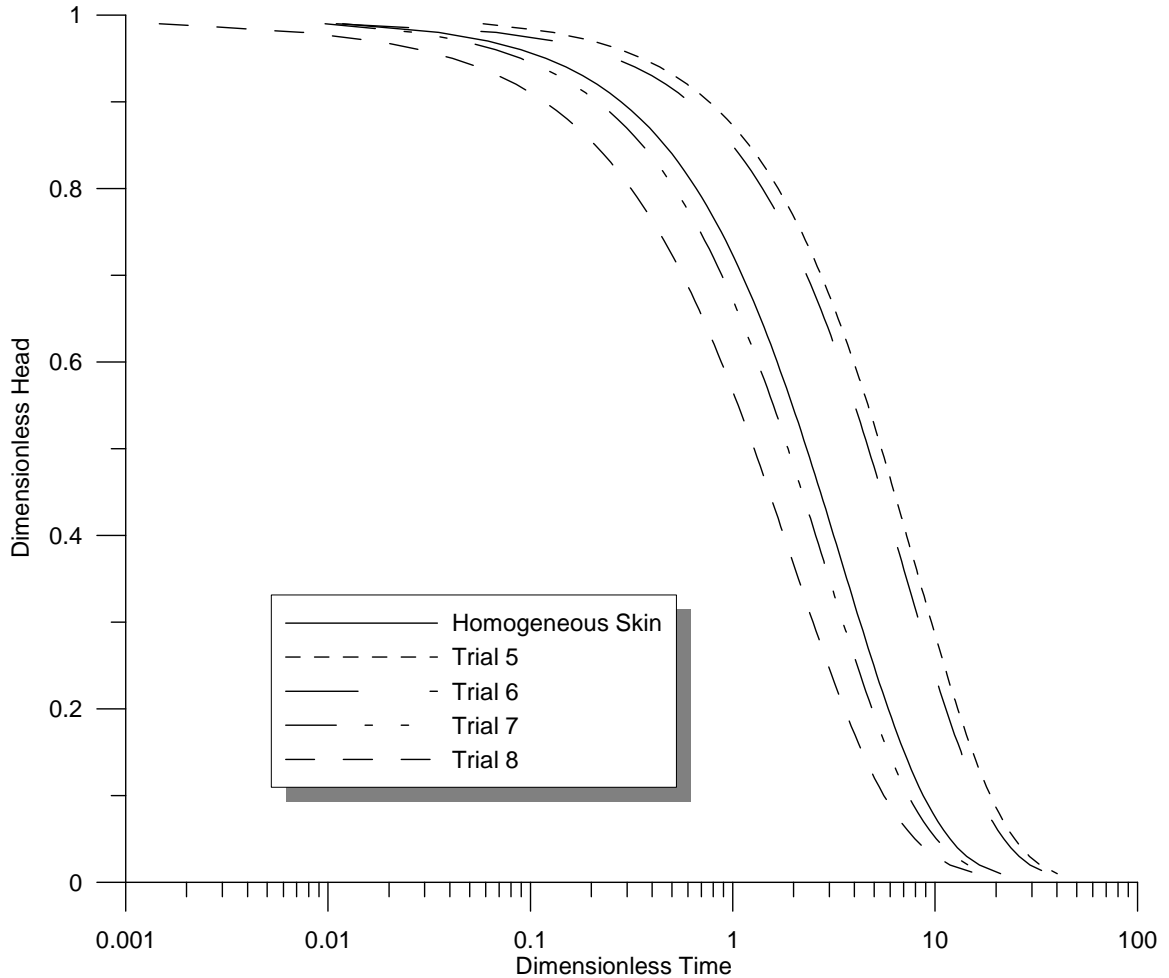


Figure 12: Normalized head versus time plots of the radial heterogeneity trials. Trials 5 and 6 show the cases when the skin is divided into 4 layers spanning the entire formation thickness while trials 7 and 8 show the effect of varying K in both the vertical and horizontal directions to produce 6 K zones.

surrounding the screen (figure 11). In these trials, conductivity within one of the screen zones is either the same value (trial 8) or one half order of magnitude lower (trial 7) than the formation conductivity. The resultant recovery curves shift to the left of the homogeneous case, indicating increased radial flow when compared to the initial two trials (figure 12).

Additional simulations were designed to quantify the impact of other skin parameters on model simulations. Trials were designed to incrementally increase the

overall thickness of the skin. Skins ranged from 5 mm up to 10 cm. The low end member was originally set at 1 mm, but the numerical model became unstable modeling flow in skin cylinders 0.1 mm in diameter. Figure 13 shows that with each successive increase in thickness, the resultant recovery curve shifts to the right. While skin thickness does have a significant impact, the number of cylinders used to simulate the skin has no affect at all. A 0.01 meter-thick skin was modeled with 2, 10, 20, and 40 meter thick aquifer using 3, 10, and 20 layers with a centered screen consisting of 1, 2, and 4 layers, respectively. All subsequent model runs showed no differences.

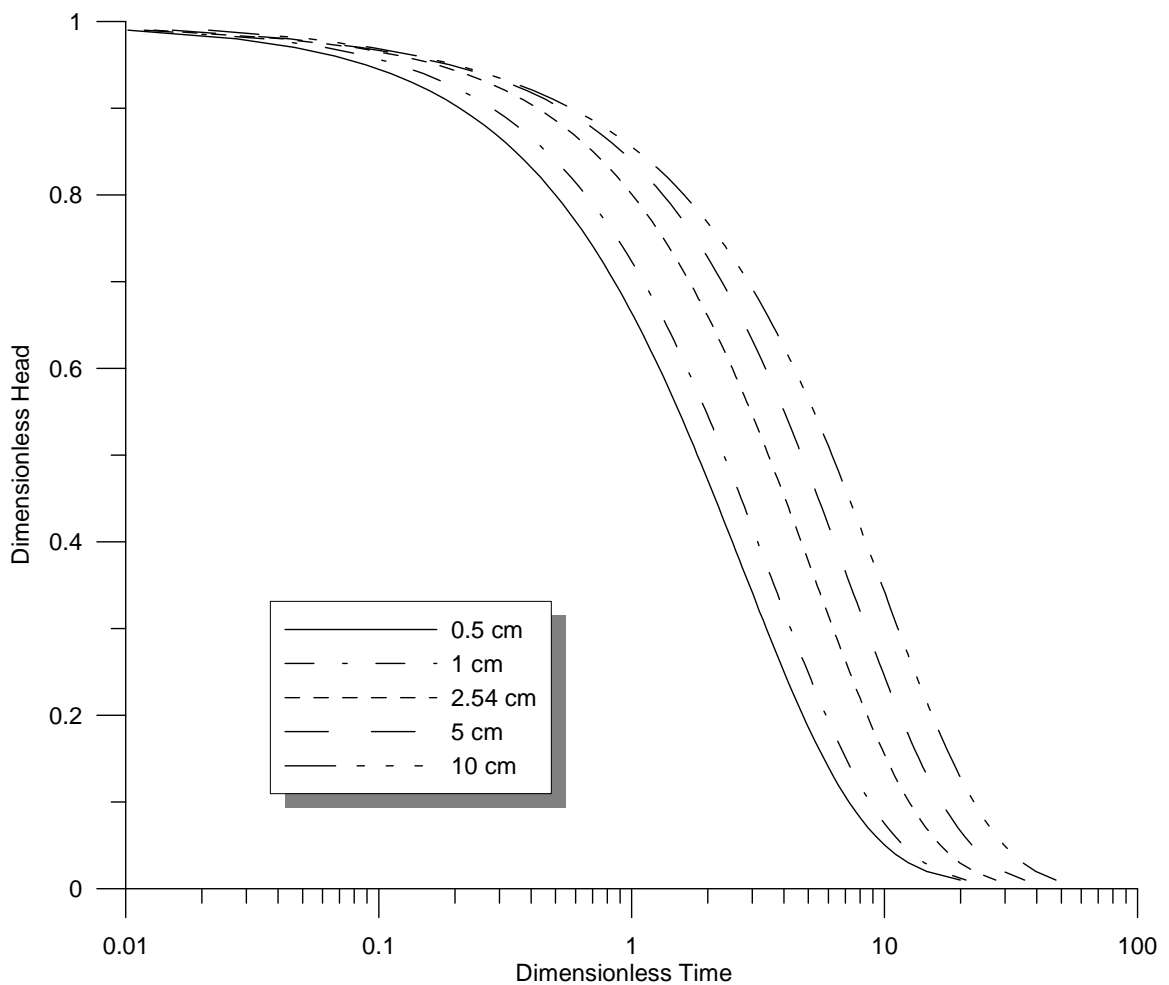


Figure 13: Normalized head versus time plots of the skin thickness trials

Partial Penetration

While the test case used in most model simulations was designed for a partially penetrating well centered in a 10 meter-thick aquifer, trials were performed to investigate the effect of varying the screen location and partial penetration factor in different types of aquifers. Initial runs utilized a thin aquifer (3 meters) consisting of three 1-meter layers with low permeability well skins. The well screen was placed in the center, at the top, and at the bottom of aquifer to see what effect screen location plays in a thin aquifer. All three numerical model runs produced identical recovery curves. Results show that if the well screen makes up a significant portion of the total thickness in a thin aquifer, radial flow overwhelms vertical flow and screen positioning is inconsequential. In the fully penetrating case, the recovery curve starts off slightly underneath the other three curves but crosses them at 60% recovery and then develops a pronounced offset at the end of the test (figure 14). Those conditions were repeated but with a shorter screen length of 0.1 meter, an order of magnitude decrease in the partial penetration factor. Recovery curves for these shorter screen length model trials are similar in the early time but deviate substantially to the left from the other curves after 10% recovery. In this case, the top and bottom curves are identical with the center curve falling to the left (figure 14).

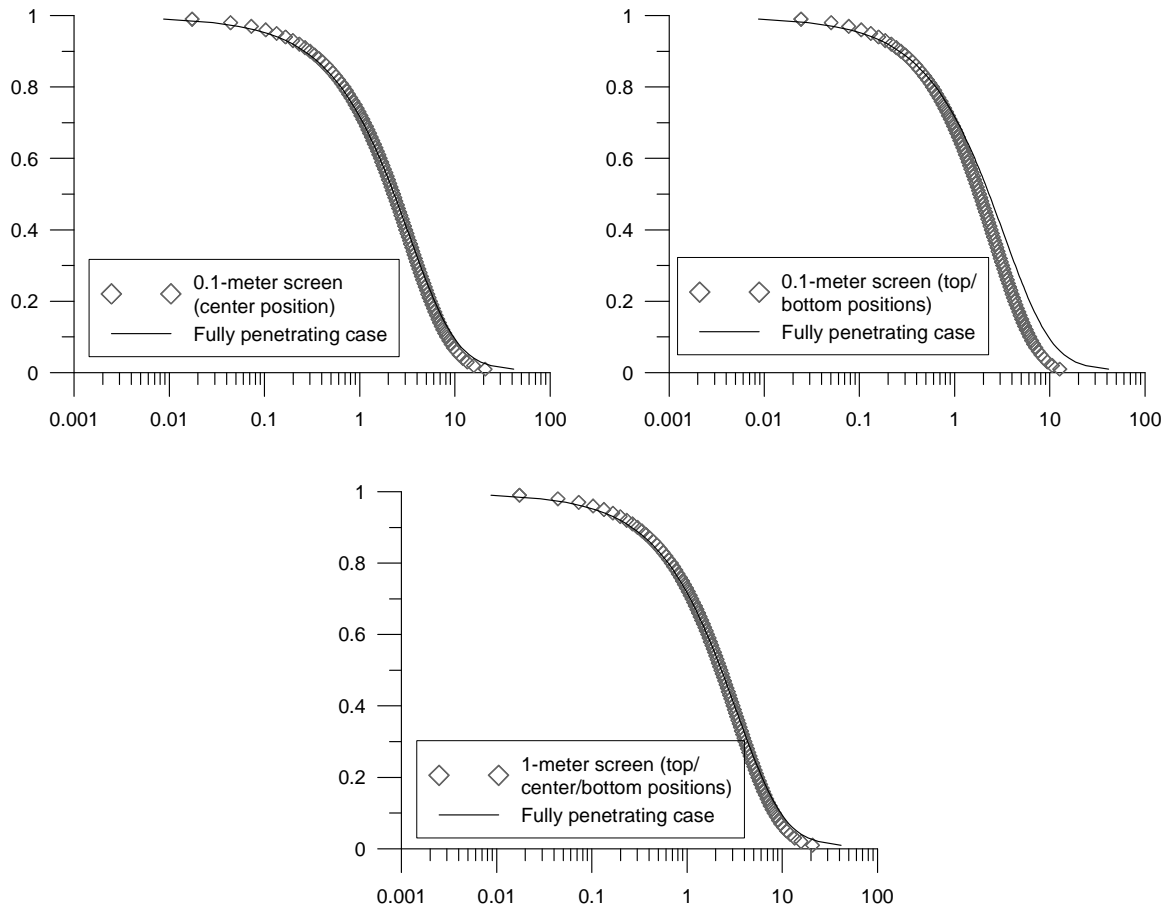


Figure 14: Normalized head versus time plots of the various partial penetration and screen location trials in a thin aquifer

A thick 35-meter aquifer with a lower permeability well skin was simulated using seven 5-meter layers with the screen in the center, the top, and the bottom. In these trials, the center and top cases were identical to the fully penetrating case. The bottom recovery curve begins on the left side of the other curves and then crosses approximately 20% into the test and stays adjacent to the other curves until it rejoins them at test completion (figure 15). Once again, the partial penetration factor was changed; this time the screen length was increased to 15 meters. These trials display the same behavior as before with identical center, top, and bottom curves (figure 15).

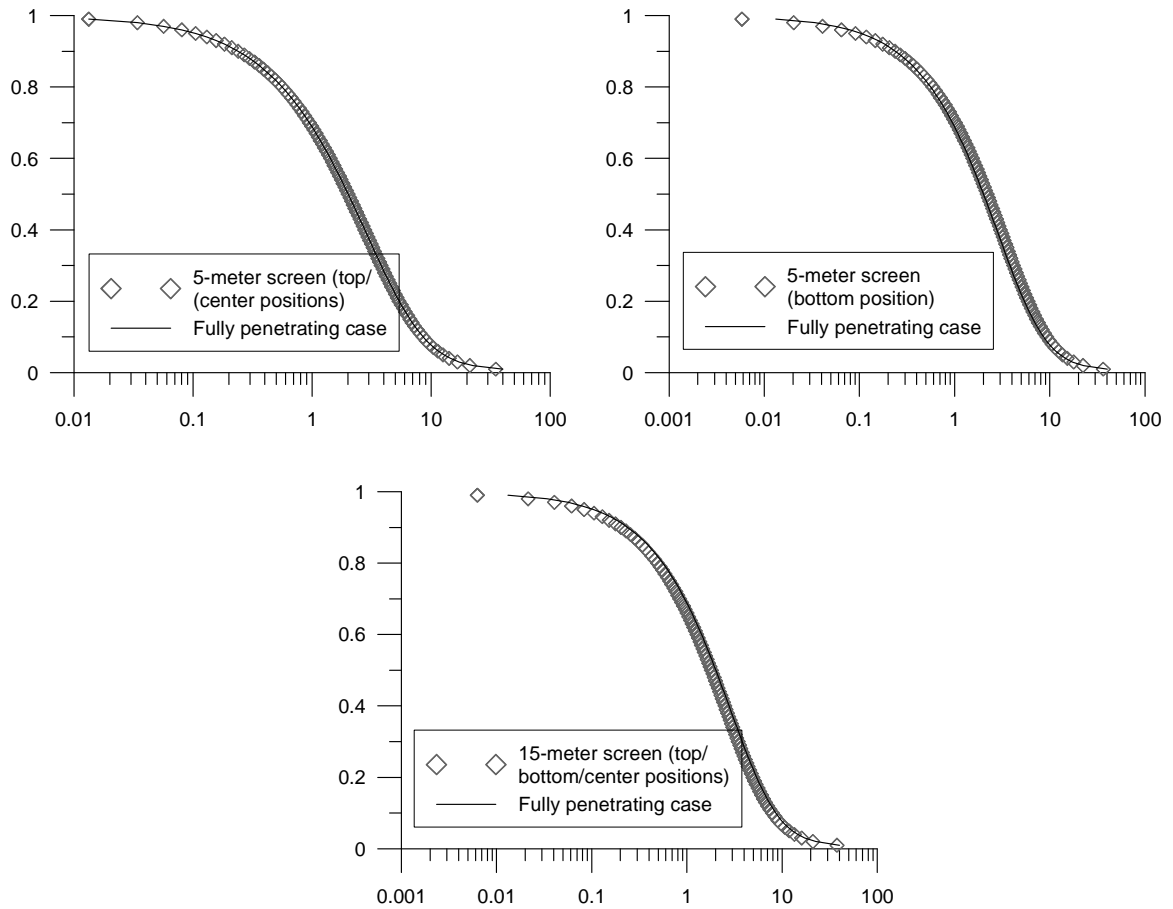


Figure 15: Normalized head versus time plots of the various partial penetration and screen location trials in a thick aquifer

Anisotropy

Various trials were developed to investigate how anisotropy in the formation, the well skin, and both affect the recovery curves. Model variables for these trials are summarized in table 3.

Table 3: Parameter values used in anisotropy STS trials

	CASE 9	CASE 10	CASE 11	CASE 12
K_R (skin)	0.00001 m/s	0.00001 m/s	0.000001 m/s	0.0001 m/s

K_V (skin)	0.00001 m/s	0.000001 m/s	0.00001 m/s	0.000001 m/s
S_S (skin)	$6.6e-3 \text{ m}^{-1}$	$6.6e-3 \text{ m}^{-1}$	$6.6e-3 \text{ m}^{-1}$	$6.6e-3 \text{ m}^{-1}$
K_R (formation)	0.0001 m/s	0.001 m/s	0.00001 m/s	0.01 m/s
K_V (formation)	0.00001 m/s	0.00001 m/s	0.0001 m/s	0.00001 m/s
S_S (formation)	$6.6e-4 \text{ m}^{-1}$	$6.6e-4 \text{ m}^{-1}$	$6.6e-4 \text{ m}^{-1}$	$6.6e-4 \text{ m}^{-1}$

The results show that if the radial and vertical conductivities of either the formation or skin are within one order of magnitude, they are identical to the isotropic case in the early time and deviate only slightly from it after about 25% completion (figure 16). The case where only the formation displays anisotropy (trial 9) falls to the right of the isotropic case and the case when both the skin and formation exhibit vertical conductivities greater than the radial component, the recovery curve plots to the left of the isotropic case.

Therefore, if the radial and vertical hydraulic conductivities are within one order of magnitude, the resultant normalized head versus time curves show minimal variations.

The difference comes in trials 10 and 12 where the formation has a radial conductivity greater than the vertical conductivity by two and three orders of magnitude, respectively.

In both of these cases, the skin also shows a one order of magnitude difference (trial 10) and a two order of magnitude difference (trial 12). In both cases, the recovery curves are shifted dramatically to the right of the other trials, indicating a significant delayed response of head in the well.

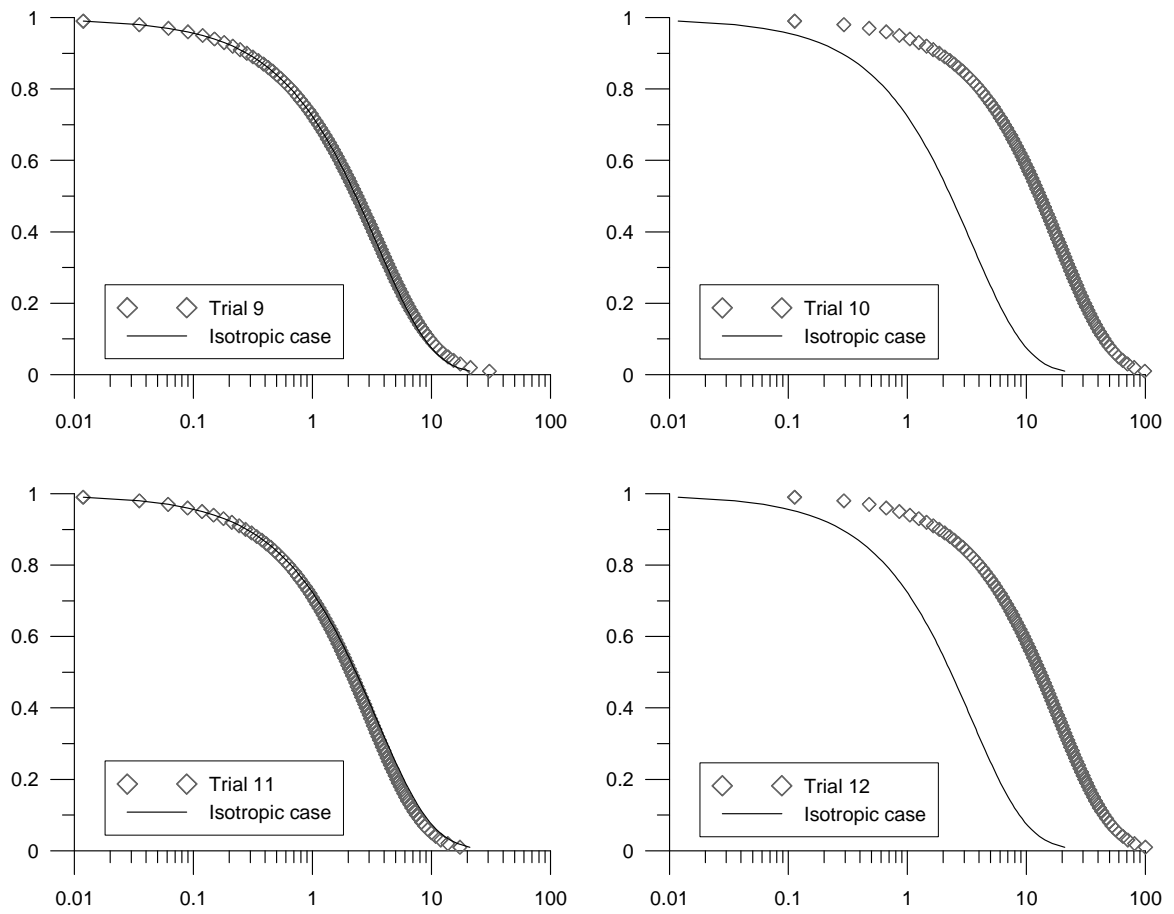


Figure 16: Normalized head versus time plots of the anisotropy trials

CHAPTER 4

DIRECT PUSH PERMEAMETER SIMULATOR (DPPS)

CYLINDRICAL FINITE-DIFFERENCE MODELING CODE

DPPS simulates two-dimensional, axially symmetrical flow created when water is injected into a specialized small-diameter direct push rod. The model consists of concentrically stacked cylinders centered on a small-diameter (0.045-meter) screen where the first cylinder is directly adjacent to the injection screen. The radius of the first cylinder was designed so that both transducers, which are located on the outside of the DPP probe, would be located at the node to accurately measure pressure (figure 17). DPPS writes the heads at both transducer locations as well as the head difference between the transducers, the cylinder radii, and heads in all of the cylinders. The mathematical foundation and Visual Basic code for the DPPS numerical model is similar in most instances to the STS numerical model described in Chapter 2. The Visual Basic code for DPPS is presented in appendix B.

DPPS versus STS

While DPPS employs the same approach as STS with respect to cylinder spacing, solution method, lower and outer boundary conditions, and the presence of a well skin, it does have several differences. STS simulates a slug test with a constant head boundary at the well adjusted at the start of each time step. The simulation continues until the head response in the well reaches a user defined recovery. However, DPPS models a small-scale injection test so the inner boundary condition has a specified flux where the total volume of water entering the formation is distributed within the layer representing the

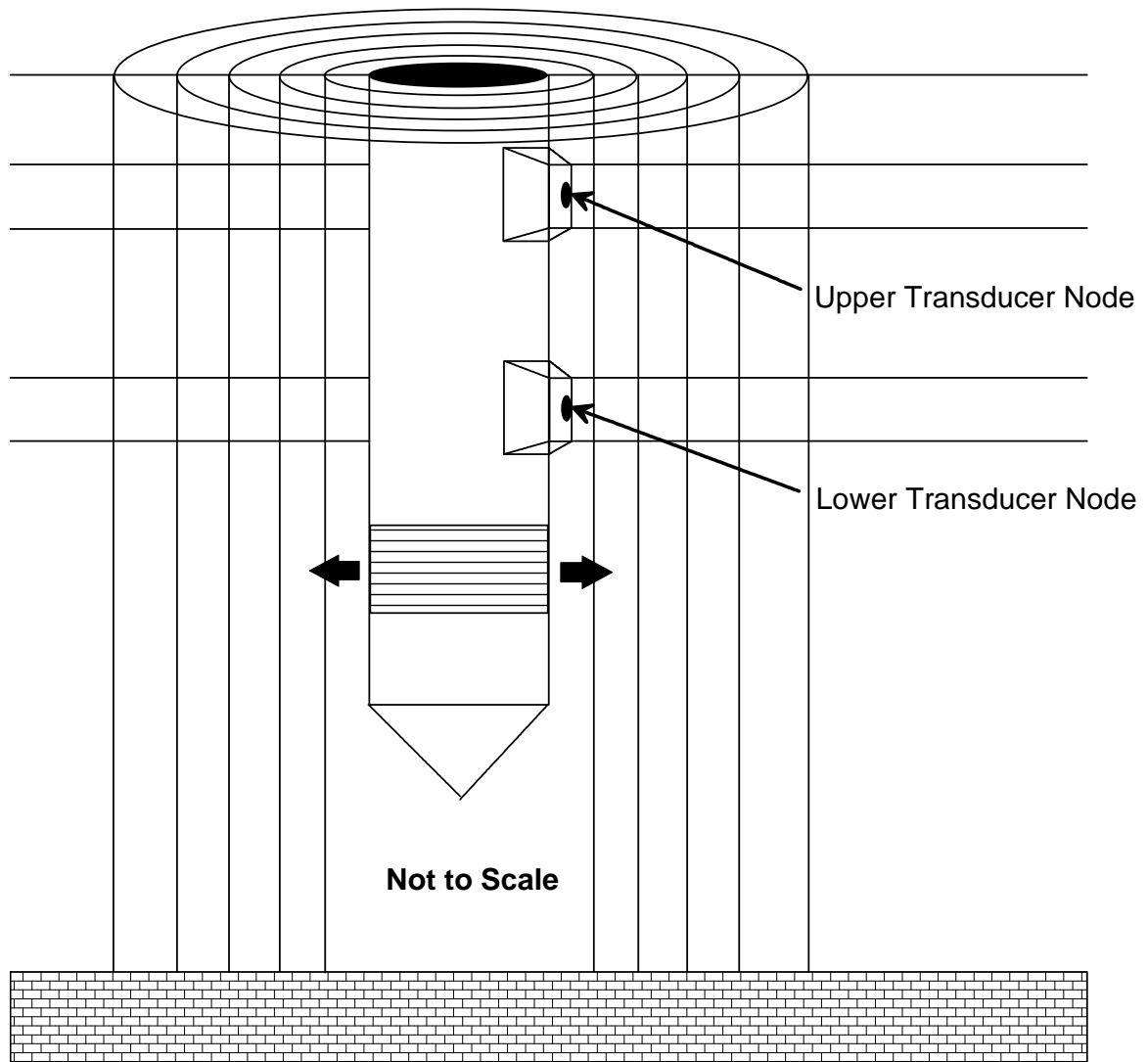


Figure 17: Conceptual model showing the cylinder design of DPPS

DPP screened interval. The volume of injected water is then added to the recharge term (R) in the governing equation.

The second main distinction between the two codes is the algorithm for creating the layers of a model. STS requires the user to input the number of layers above, within, and below the screen and calculates the thickness of each layer based on these values. Due to the smaller scale of DPP tests, layers had to remain relatively thin, particularly around the transducers where pressure is being measured. The distance from the upper

transducer to the bottom of the injection screen is constant based on instrument design at 0.4 meters with a 0.025 meter thick screen interval. Since it is this area where head measurement is especially important, all of the layers from the upper transducer to the bottom of the screen are hardwired into the code at 0.025 meters thick. The layers above and below the screen are set to 0.03 meters, a 1.2 expansion factor between adjacent layers (figure 18). This is below the recommended 1.5 maximum factor determined by Anderson and Woessner (1992) to minimize truncation errors that arise for irregular grids. In order to accomplish this, DPPS requires the user to input both the total formation thickness and the distance from the top of the aquifer or water table to the upper transducer. DPPS uses this information to calculate the number of layers above the upper transducer and the number of layers below the screened interval.

The STS code dynamically adjusts the length of each time step to maintain accuracy, and model completion depends on a user specified value for the recovery of the head in the well. For example, if the user inputs a recovery of 0.1, then the numerical model runs until the hydraulic head in the well is within 10% of the original head (or essentially when the test is 90% complete). DPPS, on the other hand, runs until a user-specified time limit is reached. The numerical code uses the same approach as that applied by McDonald and Harbaugh (1988) for MODFLOW for calculating the length of the individual time steps. The user must specify the duration of the stress period, the number of time steps within each stress period, and a time step multiplier. Using these variables, the numerical model then calculates the length of each time step using equation 40.

$$InitialTime = TestTime * \frac{(1 - Multiplier)}{1 - Multiplier^{NumberTimeSteps}} \quad (40)$$

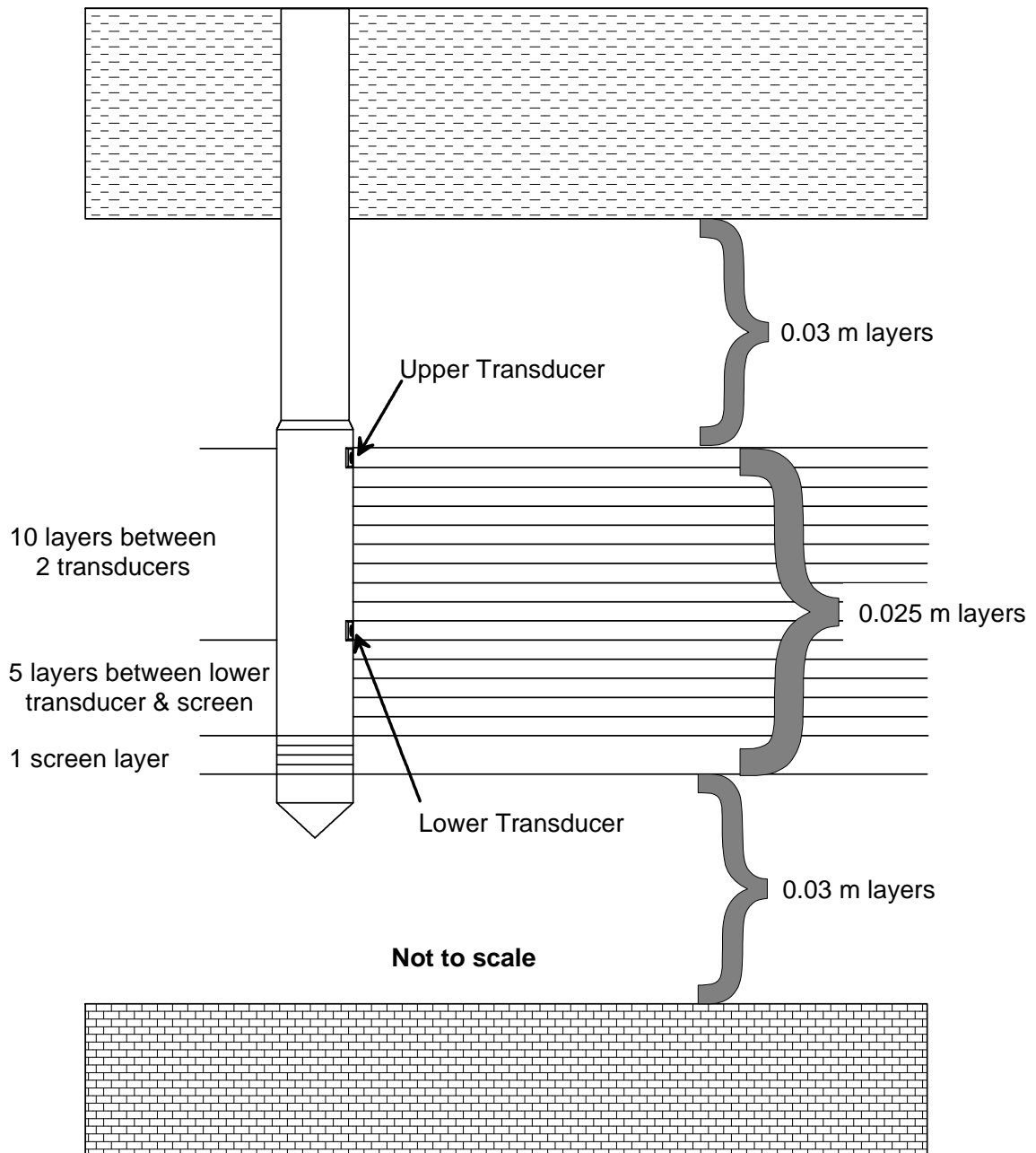


Figure 18: Conceptual model showing the layering design of DPPS

User Interface

The spreadsheet interface for DPPS has a similar design to STS (figure 19); the only difference is the addition of variables to simulate a discharge boundary rather than a constant head boundary associated with a slug test. Model variables for determining

DIRECT PUSH PERMEAMETER SIMULATOR

Geometry <input type="text" value="0.0225"/> Well casing radius <input type="text" value="0.0225"/> Well screen radius <input type="text" value="30"/> Number of cylinders	Run DPPS	Flow System <input checked="" type="radio"/> Confined <input type="radio"/> Unconfined	Model Status <input type="text" value="198.01473"/> Total time
Formation Properties <input type="text" value="10.7"/> Formation thickness <input type="text" value="7.20E-04"/> Radial hydraulic conductivity <input type="text" value="7.20E-04"/> Vertical hydraulic conductivity <input type="text" value="6.60E-04"/> Specific storage <input type="text" value="0.01"/> Specific yield (unconfined cases) <input type="text" value="7.70E-03"/> Transmissivity		Skin Properties <input type="checkbox"/> Well skin present around screen <input type="text" value=""/> Well skin radius <input type="text" value=""/> Number of skin cylinders <input type="text" value="0.01"/> Specific storage of the skin <input type="text" value="0.01"/> Specific yield of the skin (unconfined cases) <input type="checkbox"/> Homogeneous skin conductivity <input type="text" value=""/> Radial skin hydraulic conductivity <input type="text" value=""/> Vertical skin hydraulic conductivity	
Pumping Variables <input type="text" value="6.67E-05"/> Pumping rate <input type="text" value="0"/> Initial head		Model Variables <input type="text" value="0.00001"/> Tolerance <input type="text" value="0.5"/> Alpha	
Time Variables <input type="text" value="200"/> Total time of the test <input type="text" value="1.01"/> Multiplier <input type="text" value="600"/> Number of time steps		DPP Layering <input type="text" value="1.26"/> Depth from aquifer top to upper transducer	

Figure 19: DPPS spreadsheet interface for data entry

cylinder spacing within the formation and model layers are hard-wired into the code and automatically set to values that produce optimal results. The user can control model variables such as well geometry, formation properties, and time discretization. The model's running time varies based primarily on the number of layers the model generates, which in turn depends on the aquifer's saturated thickness. Simulations with thick aquifers will generate hundreds if not thousands of layers, increasing the computational time. Simulations using a thickness of 10 meters (and approximately 360 total layers) require approximately one minute to run on an Intel 3 GHz Pentium computer. The numerical model calculates the head at both transducers along with the difference in head between the transducers, allowing an easy comparison to field data.

Comparison of Model Features

DPPS has several unique features that are not found in other constant discharge test models. RADFLOW (Johnson et. al, 2000) was selected as a comparable model due

to its similar design and structure. Both DPPS and RADFLOW are finite-difference models simulating radial flow to a well, use the harmonic mean to calculate vertical conductance, and have a spreadsheet interface. While a detailed comparison is not possible since the RADFLOW's code is unavailable; a general discussion of the primary differences will be presented here.

While both RADFLOW and DPPS are finite-difference numerical models, they use different methods to generate a system of equations. RADFLOW uses a fully implicit method modified from the model developed by Prickett and Lonquist (1971) in which the head distribution is built from the heads at the previous time step utilizing a backward-difference solution technique. DPPS uses the Crank-Nicolson method, which assumes that the best approximation lies somewhere between fully implicit and explicit solutions. For this method, the hydraulic heads are calculated from a weighted average based on heads at the previous and current time steps (See Chapter 2; equation 21 for a detailed description). The Crank-Nicolson method was chosen because of its increased efficiency and accuracy (Wang and Anderson, 1982).

Another key difference is how each model handles cylinder spacing and layering. In order to determine the overall cylinder spacing, RADFLOW requires the calculation of the radius of influence as developed by Pandit and Aoun (1994):

$$R = 2\left(\frac{2.25Tt}{S}\right)^{0.5} \quad (41)$$

where T is transmissivity; t is elapsed pumping time; and S is aquifer storativity.

RADFLOW then uses this distance and the user-defined well radius to calculate its cylinder spacing, which can be fairly coarse for a large radius of influence. DPPS employs a more sophisticated logarithmic expansion methodology first developed by

Rushton and Redshaw (1979) in which the cylinders adjacent to the screen are extremely small and gradually expand as you go away from the well (See Cylinder Spacing section, Chapter 2 for details). Due to the small-scale nature of a DPP test, head measurement is most important near the well and coarse cylinder spacing can adversely affect accuracy. In respect to layers, RADFLOW places a limit of 24 layers while DPPS has no maximum, although more layers will add to the computational time required for model convergence.

The last but most important distinction between the two models is the issue of accuracy. The authors of RADFLOW estimate a maximum mean absolute error of less than 5%, which they accept as reasonable. This error may be attributed to their coarse cylinder and time spacing. The initial time step is set one order of magnitude lower than the initial drawdown with each successive time step increasing by a factor of 1 to 1.5 as determined by the user. DPPS, on the other hand, often attains model errors of 1-2% and has produced errors as low as a few tenths of a percent. In addition, when RADFLOW is validated to several analytical solutions (Theis [1935; 1940], Hantush and Jacob [1955], Hantush [1961a; 1961b], and Neuman [1974]), the comparison plots have such coarse scales that small differences between the numerical and analytical models cannot be distinguished. The validation plot of DPPS to the Theis (1935; 1940) solution is a good match with both models producing extremely similar curves (detailed description in Model Validation section below).

MODEL VALIDATION

One-dimensional and two-dimensional numerical models were compared to the Theis (1935: 1940) solution for a fully penetrating well in a confined aquifer. The final

comparison is based on a four-layer model with parameter values from an actual multiple well test presented by Wang and Anderson (1982) on an aquifer with a storativity of 0.002, a unit thickness of 10 meters, a transmissivity of $0.0035 \text{ m}^2/\text{sec}$, a pumping rate of $0.023 \text{ m}^3/\text{second}$, and an outer boundary that stretches over 8200 meters away with 100 cylinders. Figure 20 shows the agreement between the numerical and analytical solutions. The key variable in obtaining a good match is the use of a small enough initial radius so that the Theis assumption of an infinitesimal well radius is met. Any initial radius with a value greater than 0.0001 meters leads to significant errors in the comparison.

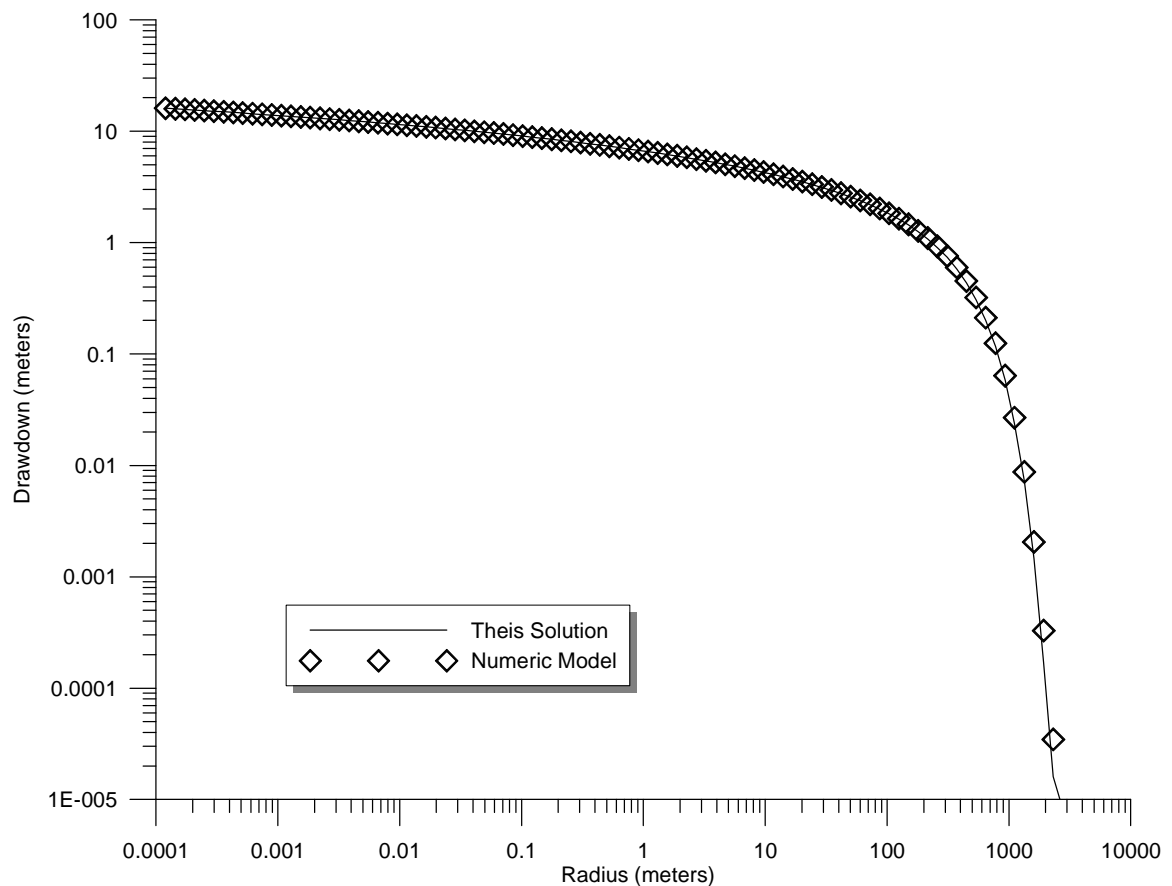


Figure 20: Validation of DPPS to the Theis analytical model

DPP FIELD DATA COMPARISON

While a good match to Theis was important, the modified simulator needed to reproduce existing DPP field data. The KGS and Geoprobe® conducted initial DPP tests at two different sites to explore the viability of the test (Butler et al., 2007). The first site, the Geohydrologic Experimental and Monitoring Site (GEMS), is located in the northeast corner of Kansas just north of Lawrence in Douglas County. This site is positioned within the Kansas River floodplain and consists of approximately 10.7 meters of coarse sand and gravel overlain by 11.5 meters of clay and silt. GEMS has been the site of numerous groundwater investigations from tracer tests to multilevel slug tests, and the spatial variations of K have been delineated with some reliability (Butler et al., 1994; 1999). The second DPP investigation was performed near Nauen, Germany in the summer of 2003. The Nauen site contains an unconfined shallow aquifer consisting of approximately 14 meters of fine to medium sands underlain by an aquiclude of clayey glacial till (Yaramanci et al., 2002). Previous investigations at the site have used several geophysical surface measurements including surface nuclear magnetic resonance, georadar, and refraction seismic as well as data from a continuously cored borehole to extensively analyze the subsurface environment (Dietrich et al., 2003).

Butler et al. (2007) provided a detailed description of the DPP tests performed at both sites and the results for each test. These values along with a comparison of the Δh values obtained from the field tests to those generated using DPPS are summarized in table 4. All values are taken from Butler et al. (2007) with the exception of specific storage values, which were estimated from the type of geologic material present and published ranges from Walton (1988) and Cheng (2000).

Table 4: Comparison of DPSS results to field data

SITE & TEST	T (M²/S)	S_s (1/M)	Q (M³/S)	ΔH (M) (FIELD DATA)	ΔH (M) (DPSS TRIAL)
GEMS #1	0.0074	6e-4	6e-5	0.0290	0.0327
GEMS #2	0.0077	6e-4	5.5e-5	0.0258	0.0298
Nauen #1	0.0022	1e-3	1.23e-5	0.026	0.0269
Nauen #2	0.0024	1e-3	2.3e-5	0.044	0.0430
Nauen #3	0.0025	1e-3	5.77e-5	0.112	0.108

When compared to the DPSS field data, the results of the numerical model show good agreement. At the GEMS site, the Δh values generated by the numerical model were slightly higher than the field data displaying an error of 12.8% for test 1 and 15.5% for test 2. The comparison involving the Nauen site was mixed with some numerical results higher than the field data and some lower. DPSS was able to match the Nauen field data with much more precision. The percent errors on the three tests were 3.5%, 2.3% and 3.6%, respectively with an average error of 3.1%.

MODEL ANALYSIS

Sensitivity Analysis

Trials were designed to investigate how specific storage, a formation property, affected DPSS. Initial results from STS model simulations showed that specific storage was a major controlling factor in the shape of the curves. Since DPSS simulates a discharge boundary, unlike STS, it was important to determine how specific storage influences the test results, since specific storage is usually not known with any certainty.

Specific storage values range between $2.6e-4$ and $2.6e-3$ m^{-1} for porous sand/sand and gravel geologic materials (Walton [1998] and Cheng [2000]). Both end members of the range were run and the difference in head between the transducers for both trials was identical, indicating that specific storage over reasonable ranges does not significantly impact DPPS simulations. The small-scale nature of DPP tests and the fact that any changes in the saturated thickness are extremely small may cause specific storage to have little impact in the test results.

Accuracy Analysis

An investigation of the accuracy of the model was conducted by varying certain user-defined model parameters including the time step multiplier, the number of time steps, and tolerance for model convergence. Conditions at the GEMS site were used to investigate the impact of changes in these variables. The confined formation has a thickness of 10.7 meters, displays the same radial and vertical hydraulic conductivity of 0.00072 m/s, and has a specific storage of $6.6e-4$ m^{-1} . While saturated thickness and conductivity were reported by Butler et al. (1994), the specific storage was selected from published ranges [Walton (1988) and Cheng (2000)] based on the type of geologic material present at the GEMS site. The injection rate used is at the upper limit for the DPP test at $6.67e-5$ m^3/s (4 liters/minute). Since a DPP test stresses such a small portion of the aquifer, only 30 cylinders were used in the simulation that lasted for 200 seconds.

Initial simulations were designed to determine a suitable tolerance for DPPS as shown in table 5. The resultant head differences only exhibit disparities three or four places past the decimal, indicating very subtle variations between trials. This may be due to the scale issue of DPP tests, stressing a very small portion of the formation, or the fact

that our numerical model is rather insensitive to tolerance. Even though the differences are minor, the resultant tolerance was chosen when two successive trials showed the least variations, and therefore a tolerance of 0.00001 was chosen for all numerical model simulations.

Table 5: Effects of tolerance on DPPS accuracy

TOLERANCE	HEAD AT UPPER TRANSDUCER	HEAD AT LOWER TRANSDUCER	HEAD DIFFERENCE (M)
0.1	0.00016068	0.0331353	0.03297462
0.01	0.00016252	0.03315118	0.03298866
0.001	0.00017056	0.03321818	0.03304762
0.0001	0.00019972	0.03343762	0.03323790
0.00001	0.00037391	0.03438012	0.03400622
0.000001	0.0006832	0.03541121	0.03472801

The last step in the accuracy analyses was to determine the optimal time step multiplier and number of time steps. In order to maximize the accuracy of the model, the time step length must be extremely small. The best way to minimize this variable is by choosing a large enough number of time steps or by choosing a suitably small time step multiplier. The larger the time step multiplier, the smaller the initial time becomes. Simulations using multipliers of 1.01, 1.005, and 1.001 all show practically the same head differences between transducers. Additional trials suggest at least 600 times steps are necessary to obtain accurate results. Increasing the number of time steps above 600 provides no additional accuracy, as shown in table 6. For the purpose of the model, 600 time steps along with a multiplier of 1.01 were determined to produce the best results.

While this combination provided optimal results, both the time step multiplier and number of time steps can be changed by the user.

Table 6: Effects of the number of time steps on DPPS accuracy

NUMBER OF TIME STEPS	HEAD AT UPPER TRANSDUCER	HEAD AT LOWER TRANSDUCER	HEAD DIFFERENCE (M)
50	0.0005994	0.0389864	0.0383870
100	0.0004779	0.0385953	0.0381174
250	0.0004543	0.0385083	0.0380539
500	0.0004480	0.0384847	0.0380367
600	0.0004469	0.0384807	0.0380338
750	0.0004465	0.0384795	0.0380329
1000	0.0004467	0.0384801	0.0380334

CHAPTER 5

CONCLUSIONS

While the straightforward nature of analytical solutions has led to their extensive use in the analysis of slug test data, their applicability to complex groundwater environments is limited. Early computers could only handle simple numerical models, but as the technology has improved, flexible numerical models have become practical. Numerical models can handle more complex conditions and can be designed on a site-specific basis, providing greater accuracy in the analysis of hydrologic tests. The cylindrical-coordinate numerical modeling codes presented in this study illustrate the increased flexibility associated with numerical solutions.

The Slug Test Simulator (STS) was designed to investigate groundwater flow in response to a slug test in porous formations. Unlike existing analytical and numerical models, STS was created with small cylinder spacing around the well and extremely small time steps for improved accuracy. STS allows certain formation properties such as hydraulic conductivity and storage to vary in both the radial and vertical directions. The code provides a simple user interface where parameters are written directly to a spreadsheet so the user can watch the progress of the model. STS was verified to the Cooper-Bredehoeft-Papadopoulos (CBP) (1967) analytical solution and the KGS (Hyder et al., 1994) semi-analytical solution for slug tests and reproduced both solutions for most cases with a high degree of accuracy.

This numerical modeling code is not ideal for all circumstances. Analytical models have distinct advantages for slug tests in relatively homogeneous formations with

no well skin or a homogeneous well skin. In the presence of a well skin, STS requires that the user has detailed knowledge of skin properties, which can never be known with any great reliability. However, trial-and-error comparisons of simulated curves with field data can provide insight on the impact of well skins on slug tests. Even in the absence of exhaustive information on well characteristics, the code described in this study has the ability to perform an exhaustive investigation of how skin properties influence head responses or to handle complex, layered heterogeneities within the groundwater system.

One of primary purposes for the development of STS was to explore how heterogeneity within a low permeability well skin would affect head response from slug tests. The results of the investigation can be summarized as follows:

1. The creation of permeable conduits within a skin through development activities can significantly lessen the effect of a positive skin on the well recovery. If any layers within the skin have the same conductivity as the surrounding formation, flow is concentrated and the resultant head response data approaches the case when no skin is present.
2. The two skin properties that have the greatest impact on the resultant recovery curves are specific storage and skin thickness.
3. When heterogeneities exist, low permeability vertical layers within the skin influence head response more than the presence of low permeability horizontal layers. This appears to be the case unless higher permeability horizontal layers exist to concentrate the flow.
4. Partial penetration plays a fairly insignificant role in slug test recovery unless the screen length is an order of magnitude lower than the total formation thickness. Screen location, whether placed at the top, center, or bottom of the formation, does not seem to

influence the resultant recovery curves when the screen's length is a large proportion of the total thickness. As the screen length decreases, the proximity of the screen to an upper or lower boundary does influence the results and a change in the recovery curve relative to the centered case for a confined aquifer.

5. Whether the skin, formation, or a combination of both are anisotropic, the normalized head versus time plots show very little variation when radial conductivity is within one order of magnitude of the vertical conductivity. In extreme situations when the skin displays two orders of magnitude difference or the radial conductivity in the formation is two to three orders of magnitude greater than the vertical conductivity, then a dramatic shift of the recovery curves can be attributed to larger vertical components of flow.

This research indicates that while some skin properties have little effect on the response of a slug test, others greatly influence the test and can lead to significant errors in the value of hydraulic conductivity. While some skin properties (specific storage, thickness, conductivity distribution) are usually unknown, drilling logs and sediment samples can at least produce viable ranges for some of the unknowns. Even if some of the skin characteristics are unknown, STS allows the user to systematically vary parameter input to match the recovery curve to field data. While this feature allows the user to explore various combinations of parameters, the possibility for a non-unique solution arises. While having a limited range of parameter values can decrease the chance for a non-unique solution, the best approach to minimize or even eliminate the well skin effect is to ensure proper development and periodic cleaning of the well screen.

Inherent limitations associated with slug test methodology have led to research on new direct-push methodology for determining formation properties. The Kansas

Geological Survey has developed one such field technique, the Direct-Push Permeameter (DPP), designed to overcome the presence of fine-grained material generated during pushing activities. Because of the lack of existing analytical or numerical models that could specifically simulate the unique mechanics and geometry of DPP tests, another numerical modeling code, the Direct-Push Permeameter Simulator (DPPS), was created through modifications of the original STS code. DPPS has many of the same features incorporated into STS including the ability to handle partial penetration, well skins, and layered heterogeneities with simple spreadsheet data entry and graphical display. While the two numerical models are similar, DPPS was designed to simulate a constant discharge test with much thinner horizontal layers. DPPS reproduced the Theis (1935; 1940) solution while also matching existing DPP field data.

Trials were designed to determine the overall impact of several key user-defined model parameters on the accuracy of the model. An in-depth investigation of the influence of tolerance, time step multiplier, and number of time steps led to a determination of their optimal values, which are 0.00001, 1.01, and 600, respectively. In order to determine these values, each parameter was adjusted until the head differences between the upper and lower pressure transducers were almost indistinguishable.

Agreement between data collected in the field and numerical model simulations show that the DPP methodology has merit. The numerical model was able to reasonably recreate DPP field data conducted at two sites with distinctly different media properties. The GEMS and Nauen sites had an average error of 14.2% and 3.1%, respectively between the field data and DPPS simulations. While the comparisons are not exact matches, this discrepancy might be due to the fact that specific storage was estimated

from published values; more accurate field measurements of storage might improve model results. Additional research is being conducted by the KGS in order to fully explore and refine the DPP methodology.

REFERENCES

- Anderson, M.P. and Woessner, W.W., 1992. Applied groundwater modeling---
Simulation of flow and advective transport: Academic Press, San Diego, CA.
- Bjerg, P.L., Hinsby, K., Christensen, T.H., and Gravesen, P., 1992. Spatial variability of hydraulic conductivity of an unconfined sandy aquifer determined by a mini slug test. *Journal of Hydrology*, 136: 107-122.
- Bohling, G.C. and Butler, J.J., Jr., 2001. lr2dinv: A finite-difference model for inverse analysis of two-dimensional linear or radial groundwater flow. *Computers and Geosciences*, 27(10): 1147-1156.
- Bouwer, H. and Rice, R.C., 1976. A slug test for determining hydraulic conductivity of unconfined aquifers with completely or partially penetrating wells. *Water Resources Research*, 12: 423-428.
- Brown, D.L., Narasimhan, T.N., and Demir, Z., 1995. An evaluation of the Bouwer and Rice method of slug test analysis. *Water Resources Research*, 31(5): 1239-1246.
- Butler, J.J., Jr., 1990. The role of pumping tests in site characterization: Some theoretical considerations. *Ground Water* 28(3): 394-402.
- Butler, J.J., Jr., 1998. *The Design, Performance, and Analysis of Slug Tests*. Lewis Publishers, Florida.
- Butler, J.J., Jr. and Healey, J.M., 1998. Relationship between pumping-test and slug-test parameters: Scale effect or artifact? *Ground Water*, 36(2): 305-313.

- Butler, J.J., Jr., Bohling, G.C., Hyder, Z., and McElwee, C.D., 1994. The use of slug tests to describe vertical variations in hydraulic conductivity. *Journal of Hydrology*, 156: 137-162.
- Butler, J.J., Jr., McElwee, C.D., and Liu, W., 1996. Improving the quality of parameter estimates obtained from slug tests. *Ground Water*, 34(3):480-490.
- Butler, J.J. Jr., McElwee, C.D., and Bohling, G.C., 1999. Pumping tests in networks of multilevel sampling wells: Motivation and methodology. *Water Resources Research*, 35(11): 3553-3560.
- Butler, J.J. Jr., Healey, J.M., McCall, G.W., Garnett, E.J., and Loheide, S.P., 2002. Hydraulic tests with direct-push equipment. *Ground Water*, 40(1): 25-36.
- Butler, J.J., Jr., Dietrich, P., Wittig, V., and Christy, T., 2007. Characterizing hydraulic conductivity with the direct-push permeameter. *Ground Water*, 45(4): 409-419.
- Cassiani, G., Kabala, Z.J., and Medina, M.A., Jr., 1999. Flowing partially penetrating well: solution to a mixed-type boundary value problem. *Water Resources Research*, 23: 59-68.
- Chen, C.S. and Chang, C.C., 2003. Well hydraulics theory and data analysis of the constant head test in an unconfined aquifer with the skin effect. *Water Resources Research*, 39(5): 1121, doi:10.1029/2002WR001516.
- Cheng, A.H.D., 2000. *Multilayered Aquifer Systems: Fundamentals and Applications*. Marcel Dekker, Inc., New York.
- Chiu, P. Y., Yeh, H.D., and Yang, S.Y., 2007. A new solution for a partially penetrating constant-rate pumping well with a finite-thickness skin. *International journal for numerical and analytical methods in geomechanics*, 31(15): 1659-1674.

- Cho, J.S., Wilson, J.T., and Beck, F.P., Jr., 2000. Measuring vertical profiles of hydraulic conductivity with in situ direct-push methods. *Journal of Environmental Engineering*, 126(8): 775-777.
- Cooper, H.H. Jr., Bredehoeft, J.D., and Papadopoulos, I.S., 1967. Response of a finite-diameter well to an instantaneous change of water. *Water Resources Research*, 3(1): 263-269.
- Dagan, G., 1978. A note on packer, slug, and recovery tests in unconfined aquifers. *Water Resources Research*, 14(5): 929-934.
- Demir, Z., and Narasimhan, T.N., 1994. Improved interpretation of Hvorslev tests. *Journal of Hydraulic Engineering*, 120(4): 477-494.
- Dietrich, P., Butler, J.J., Jr., Yaramanci, U., Wittig, V., Tiggelmann, T., and Schoofs, S., 2003. Field comparison of direct-push approaches for determination of K-profiles (abstract), *Eos*, 84(46): F661.
- Faust, C.R. and Mercer, J.W., 1984. Evaluation of slug tests in wells containing a finite-thickness skin. *Water Resources Research*, 20(4): 504-506.
- Ferris, J.G., and Knowles, D.B., 1954. The slug test for estimating transmissibility. U.S. Geological Survey Ground Water Note, 26: 1-7.
- Fetter, C.W., 2001. *Applied Hydrogeology*, 4th Edition. Prentice Hall, New Jersey.
- Hantush, M.S., 1956. Analysis of data from pumping tests in leaky aquifers. *Transactions, American Geophysical Union*, 37: 702-714.
- Hantush, M.S., 1961a. Drawdown around a partially penetrating well. *J. Hydraul. Div. Am. Soc. Civ. Eng.*, 87(HY4): 83-98.

- Hantush, M.S. 1961b. Aquifer tests on partially penetrating wells. *Journal of the Hydraulics Division, Proceedings of the Am. Soc. of Civil Eng.* 87, no. HY4: 83-98.
- Hantush, M.S. and Jacob, C.E., 1954. Plane potential flow of ground-water with linear leakage. *Transactions, American Geophysical Union Transactions*, 35: 917-936.
- Hantush, M.S. and Jacob, C.E., 1955. Non-steady radial flow in an infinite leaky aquifer. *American Geophysical Union Transactions*, 36:95-100.
- Hayashi, K., Ito, T., and Abe, H., 1987. A new method for the determination of in situ hydraulic properties by pressure pulse tests and application to the Higashi Hachimantai geothermal field. *Journal of Geophysical Research*, 92(B9): 9168-9174.
- Henebry, B.J. and Robbins, G.A., 2000. Reducing the influence of skin effects on hydraulic conductivity determinations in multilevel samplers installed with direct push methods. *Ground Water*, 38(6): 882-886.
- Hinsby, K., Bjerg, P.L., Andersen, L.J., Skov, B., and Clausen, E.V., 1992. A mini slug test method for determination of a local hydraulic conductivity of an unconfined sandy aquifer. *Journal of Hydrology*, 136: 87-106.
- Hurst, W., 1953. Establishment of the skin effect and its impediment to fluid flow into a well bore. *Petroleum Engineering*, 25: B6-16.
- Hvilshoj, S., Jensen, K.H., and Madsen, B., 2000. Single-well dipole flow tests: Parameter estimation and field testing. *Ground Water*, 38(1): 53-62.
- Hvorslev, M.J., 1951. Time lag and soil permeability in ground-water observations. US Army Corps Eng. *Waterways Exp. St. Bull.* 36, 50 pp.

- Hyder, Z. and Butler, J.J., Jr., 1995. Slug tests in unconfined formations: An assessment of the Bouwer and Rice technique. *Ground Water*, 33(1): 16-22.
- Hyder, Z., Butler, J.J., Jr., McElwee, C.D., Liu, W., 1994. Slug tests in partially penetrating wells. *Water Resources Research*, 30(11), 2945-2957.
- Johnson, G.S., Cosgrove, D.M., and Frederick, D.B., 2001. A numerical model and spreadsheet interface for pumping test analysis. *Ground Water*, 39(4): 582-592.
- Kabala, Z.J., 1993. The Dipole Flow Test: A new single-borehole test for aquifer characterization. *Water Resources Research*, 29(1): 99-107.
- McCall, W., Butler, J.J., Jr., Healey, J.M., Lanier, A.A., Sellwood, S.M., and Garnett, E.J., 2002. A dual-tube direct-push method for vertical profiling of hydraulic conductivity in unconsolidated formations. *Environmental & Engineering Geoscience*, 8(2): 75-84.
- McDonald, M.G. and Harbaugh, A.W., 1988, A Modular Three Dimensional Finite-Difference Groundwater Flow Model: U.S. Geological Survey Open File Report 83-875, Denver, CO.
- McElwee, C.D., Butler, J.J., Jr., Liu, W., and Bohling, G.C., 1990. Effects of partial penetration, anisotropy, boundaries and well skin on slug tests. *Kansas Geological Survey Report No. 91-13*.
- Melville, J.G., Molz, F.J., Guven, O., and Widdowson, M.A., 1991. Multilevel slug tests with comparisons to tracer data. *Ground Water*, 29(6): 897-907.
- Moench, A.F. and Hsieh, P.A., 1985. Comment on "Evaluation of slug tests in wells containing a finite-thickness skin," *Water Resources Research*, 21(9): 1459-1461.

- Neuman, S.P., 1974. Effect of partial penetration on flow in unconfined aquifers considering delayed gravity response. *Water Resources Research*, 10(2): 303-312.
- Neuman, S.P., 1975. Analysis of pumping test data from anisotropic unconfined aquifers considering delayed gravity response. *Water Resources Research*, 11(2): 329-342.
- Novakowki, K.S., 1989. A composite analytical model for analysis of pumping tests affected by well bore storage and finite thickness skin. *Water Resources Research*, 25(9): 1937-1946.
- Pandit, A. and Aoun, J.M., 1994. Numerical modeling of axisymmetric flow. *Ground Water*, 32(3): 458-464.
- Papadopoulos, I.S., Bredehoeft, J.D., and Cooper, H.H., Jr., 1973. On the analysis of "slug test" data. *Water Resources Research*, 9(4): 1087-1089.
- Prickett, T.A. and Lonquist, C.G., 1971. Selected digital computer techniques for ground water resource evaluation. *Illinois State Water Survey Bulletin* 55.
- Ramey, H.J., Jr., Agarwal, R.G., and Martin, I., 1975. Analysis of "Slug Test" or DST flow period data. *Journal of Canadian Petroleum Technology*, 14(3): 37-47.
- Rathod, K.S. and K.R. Rushton. 1984. Numerical method of pumping test analysis using microcomputers. *Ground Water*, 22(5): 602-608.
- Rathod, K.S. and Rushton, K.R., 1991. Interpretation of pumping from two-zone layered aquifers using a numerical model. *Ground Water*, 29(4): 499-509.
- Reilly, T.E., and Harbaugh, A.W., 1993. Simulation of cylindrical flow to a well using the U.S. Geological Survey Modular Finite-Difference Ground-Water Flow Model. *Ground Water* 31(3), 489-494.

- Rushton, K.R. and Booth, S.J., 1976. Pumping-test analysis using a discrete time-discrete space numerical method. *Journal of Hydrology*, 28: 13-27.
- Rushton, K.R. and Chan, Y.K., 1976. Pumping test analysis when parameters vary with depth. *Ground Water*, 14(2): 82-87.
- Rushton, K.R. and Redshaw, S.C., 1979. *Seepage and Groundwater Flow: Numerical Analysis by Analog and Digital Methods*. John Wiley & Sons, Great Britain.
- Rutledge, A.T., 1991. An axisymmetric finite-difference flow model to simulate drawdown in and around a pumped well. USGS Water Resources Investigations Report 90-4098.
- Springer, R.K. and Gelhar, L.W., 1991. Characterization of large scale aquifer heterogeneity in glacial outwash by analysis of slug tests with oscillatory response, Cape Cod, Massachusetts. In: G. Mallard and D. Aronson (Eds.), U.S. Geological Survey, Toxic Substances Hydrology Program, Proceeding of the Technical Meeting, Monterey, California, March 11-15, 1991, USGS, WRI Rept. 91-4034, Reston, Virginia, 36-40
- Sudicky, E.A., 1986. A natural gradient experiment on solute transport in a sand aquifer. Spatial variability of hydraulic conductivity and its role in the dispersion process. *Water Resources Research*, 22: 2069-2082.
- Taylor, K., Wheatcraft, S., Hess, J., Hayworth, J., and Molz, F., 1990. Evaluation of methods for determining the vertical distribution of hydraulic conductivity. *Ground Water*, 28(1): 88-98.
- Thiem, G., 1906. *Hydrologische methoden*. Leipzig, Gebhardt.
- Theis, C.V., 1935. The lowering of the piezometer surface and the rate and discharge of a

- well using ground-water storage. Transactions, American Geophysical Union, 16: 519-524.
- Theis, C.V., 1940. The source of water derived from wells—essential factors controlling the response of an aquifer to development. Civil Eng., American Society of Civil Engineers: 277-280.
- United States Environmental Protection Agency (USEPA), 1997. Expedited Site Assessment Tools for Underground Storage Tank Sites, EPA/510/B-97/001. Office of Underground Storage Tanks, Washington, DC.
- van Everdingen, A.F., 1953. The skin effect and its influence in the productive capacity of a well. Transactions, AIME 198: 171-176.
- van Everdingen, A.F., and Hurst, W., 1949. The application of the Laplace transformation to flow problems in reservoirs. Trans. Am. Inst. Min. Metall. Pet. Eng., 186: 305-324.
- Walton, W.C., 1988. Practical Aspects of Ground Water Modeling. Worthington, Ohio. National Water Well Association.
- Wang, H.B. and Anderson, M.P., 1982. Introduction to groundwater modeling: Finite difference and finite element methods. W.H. Freeman and Company, New York.
- Widdowson, M.A., Molz, F.J., and Melville, J.G., 1990. An analysis technique for multilevel and partially penetrating slug test data. Ground Water, 28(6): 937-945.
- Yang, Y. J. and Gates, T.M., 1997. Wellbore skin effect in slug-test data analysis for low-permeability geologic materials. Ground Water, 35(6): 931-937.
- Yaramanci, U., Lange, G., and Hertrich, M., 2002. Aquifer characterization using Surface NMR jointly with other geophysical techniques at the Nauen/Berlin test site.

Journal of Applied Geophysics, 50: 47-65.

Zhang, Y. and Neumann, S.P., 1990. A quasi-linear theory of non-Fickian and Fickian subsurface dispersion 2. Application to anisotropic media and the Borden site.

Water Resources Research, 26: 903-913.

Zlotnik, V.A. and Ledder, G., 1996. Theory of dipole flow in uniform anisotropic aquifers. Water Resources Research, 32(4): 1119-1128.

Zlotnik, V.A. and McGuire, V.L., 1998. Multi-level slug test in highly permeable formations: 1. Modification of the Springer-Gelhar (SG) model. Journal of Hydrology, 204: 271-282.

Zlotnik, V.A., Zurbuchen, B.R., and Ptak, T., 2001. The steady-state dipole-flow test for characterization of hydraulic conductivity statistics in a highly permeable aquifer: Horkheimer Insel Site, Germany. Ground Water, 39(4): 504-516.

APPENDICES

APPENDIX A
STS Visual Basic Code

Option Explicit

Public Const Pi As Double = 3.14159265358979

Public NewHead() As Double

Public OldHead() As Double

Public Radius() As Double

Public Edge() As Double 'only used for the block-centered approach

Public Volume() As Double

Public Area() As Double

Public Thickness() As Double

Public Elevation() As Double

Public Status() As Long

Public Base As Double

'the elevation of the bottom of the flow system

Public KRT() As Double

Public KZT() As Double

Public KR2AR() As Double

Public KZ2AR() As Double

Public KR1 As Double

Public KZ1 As Double

Public KR2 As Double

Public KZ2 As Double

Public InitialHead As Double

Public WellHead As Double

Public OldWellHead As Double

Public DWellHead As Double

Public CumulativeTime As Double

Public Recovery As Double

Public WellGradient As Double

Public Tolerance As Double

Public Maximum As Double

Public Stress As Double

Public StressHead As Double

Public ReservoirArea As Double

Public CellFlowVolume As Double

Public WellFlowVolume As Double

Public WellConductance As Double

Public Gradient As Double

Public AA() As Double

Public WellRadius As Double

Public CasingRadius As Double
 Public Time As Double
 Public DTime As Double
 Public Target As Double
 Public AnotherTarget As Double
 Public Difference As Double
 Public Alpha As Double
 Public G As Double
 Public PerComp As Double

Public I As Long
 Public J As Long
 Public Layers As Long
 Public Cylinders As Long
 Public SkinCylinders As Long

Public SkinRadius As Double
 Public SkinCellWidth As Double 'this is a uniform number for each cell in the skin
 Public Index As Long
 Public Counter As Long
 Public Step As Long
 Public Iteration As Long

Public FirstCall As Boolean

Public Cr() As Double
 Public Cv() As Double

Public Ktype As Double

Public B As Double
 Public B1 As Double 'variables for layers, parallel those of KGS
 Public B2 As Double 'variables for layers, parallel those of KGS
 Public NU As Long
 Public NS As Long
 Public NL As Long

Public Storage() As Double
 Public S1() As Double
 Public S2() As Double
 Public ST2() As Double
 Public SY1 As Double
 Public SY2 As Double
 Public FS As Long
 Public LS As Long

Public RowCounter As Long

Public Old As Double

Public Error As Double

Public InnerOldHead As Double

Public OuterOldHead As Double

Public InnerNewHead As Double

Public OuterNewHead As Double

Public UpOldHead As Double

Public DownOldHead As Double

Public UpNewHead As Double

Public DownNewHead As Double

Public CenterOldHead As Double

Public Temporary As Double

Public D As Double

Public E As Double

Public InnerC As Double

Public OuterC As Double

Public UpperC As Double

Public LowerC As Double

Public Confined As Integer

Public Skin As Boolean

Public Homogeneous As Boolean

Public LayerProperties As Boolean

Public ISKIN As Long

Public HOMOSKIN As Long

Public LAYPROP As Long

Public DataSheet As Worksheet

Public Results As Worksheet

Public Conductivity As Worksheet

Sub InitializeModel()

'Set the names of the sheets that will be used for input/output

Set DataSheet = Worksheets("Data Entry")

Set Results = Worksheets("Well Results")

Set Conductivity = Worksheets("Conductivity")

'Set model geometry

WellRadius = DataSheet.Cells(5, 3).Value

CasingRadius = DataSheet.Cells(6, 3).Value

Cylinders = DataSheet.Cells(7, 3).Value

'Set saturated thickness

B = DataSheet.Cells(13, 3).Value

'Set screen characteristics

B1 = DataSheet.Cells(22, 3).Value 'depth from top of aquifer to top of screen

B2 = DataSheet.Cells(23, 3).Value 'screen length

NU = DataSheet.Cells(24, 3).Value 'number of layers above the screen

NS = DataSheet.Cells(25, 3).Value 'number of layers in the screened interval

NL = DataSheet.Cells(26, 3).Value 'number of layers below the screen

Layers = NU + NS + NL

'Setting the size of all of the arrays

ReDim Radius(1 To Cylinders)

ReDim Edge(1 To Cylinders)

ReDim NewHead(1 To Layers, 1 To Cylinders)

ReDim OldHead(1 To Layers, 1 To Cylinders)

ReDim Thickness(1 To Layers, 1 To Cylinders)

ReDim Elevation(1 To Layers)

ReDim Volume(1 To Layers, 1 To Cylinders)

ReDim Status(1 To Layers, 1 To Cylinders)

ReDim Cr(1 To Layers, 1 To Cylinders)

ReDim Cv(1 To Layers, 1 To Cylinders)

ReDim Area(1 To Cylinders)

ReDim AA(1 To Cylinders)

ReDim KRT(1 To Layers, 1 To Cylinders)

ReDim KZT(1 To Layers, 1 To Cylinders)

ReDim KR2AR(1 To Layers)

ReDim KZ2AR(1 To Layers)

ReDim ST2(1 To Layers)

ReDim S1(1 To Layers, 1 To Cylinders)

ReDim S2(1 To Layers, 1 To Cylinders)

ReDim Storage(1 To Layers, 1 To Cylinders)

'Setting the values of the check buttons/boxes

Confined = DataSheet.Cells(1, 50).Value

Skin = DataSheet.Cells(2, 50).Value

Homogeneous = DataSheet.Cells(3, 50).Value

LayerProperties = DataSheet.Cells(4, 50).Value

If Skin Then ISKIN = 1 Else ISKIN = 0

If Homogeneous Then HOMOSKIN = 1 Else HOMOSKIN = 0

If LayerProperties Then LAYPROP = 1 Else LAYPROP = 0

'Set hydraulic head parameters

InitialHead = DataSheet.Cells(31, 3).Value

Stress = DataSheet.Cells(32, 3).Value

StressHead = InitialHead + Stress

'Set model variables

Time = DataSheet.Cells(25, 11).Value

Tolerance = DataSheet.Cells(26, 11).Value

Recovery = DataSheet.Cells(27, 11).Value 'Completion of test (0.1 indicates
90% recovery)

Alpha = DataSheet.Cells(28, 11).Value

'If user inputs no skin, then for code to work, we are setting 1 skin cell with the
'same hydraulic conductivity as formation in order to set locations of
'corresponding nodes

If ISKIN = 0 Then

 SkinCylinders = 1

 SkinCellWidth = 0.01

Else

 SkinRadius = DataSheet.Cells(12, 11).Value

 SkinCylinders = DataSheet.Cells(13, 11).Value

 SkinCellWidth = (SkinRadius - WellRadius) / SkinCylinders

End If

GenerateGeometry

'Loop to set storage and hydraulic conductivity if no skin present and have
'homogeneous formation properties

If ISKIN = 0 And LAYPROP = 1 Then

 For I = 1 To Layers

 For J = 1 To Cylinders

 S2(I, J) = DataSheet.Cells(16, 3).Value

 S1(I, J) = S2(I, J)

 KR2 = DataSheet.Cells(14, 3).Value

 KR1 = KR2

 KRT(I, J) = 2 * Pi * KR2 / AA(J)

 KZ2 = DataSheet.Cells(15, 3).Value

 KZ1 = KZ2

 KZT(I, J) = 2 * Area(J) * KZ2

 Next

 Next

End If

```

'Loop to set storage and hydraulic conductivity if no skin present and have
'heterogeneous formation properties
If ISKIN = 0 And LAYPROP = 0 Then
    For I = 1 To Layers
        For J = 1 To Cylinders
            S2(I, J) = Worksheets("Layer Properties").Cells(I + 7,
            4).Value
            S1(I, J) = S2(I, J)
            KR2 = Worksheets("Layer Properties").Cells(I + 7,
            2).Value
            KR1 = KR2
            KRT(I, J) = 2 * Pi * KR2 / AA(J)
            KZ2 = Worksheets("Layer Properties").Cells(I + 7,
            3).Value
            KZ1 = KZ2
            KZT(I, J) = 2 * Area(J) * KZ2
        Next
    Next
End If

'Loop to set storage and hydraulic conductivity in skin when skin is present
If ISKIN = 1 And HOMOSKIN = 1 Then
    For I = 1 To Layers
        For J = 1 To SkinCylinders
            S1(I, J) = DataSheet.Cells(14, 11).Value
            KR1 = DataSheet.Cells(19, 11).Value
            KRT(I, J) = 2 * Pi * KR1 / AA(J)
            KZ1 = DataSheet.Cells(20, 11).Value
            KZT(I, J) = 2 * Area(J) * KZ1
        Next
    Next
End If

If ISKIN = 1 And HOMOSKIN = 0 Then
    For I = 1 To Layers
        For J = 1 To SkinCylinders
            S1(I, J) = DataSheet.Cells(14, 11).Value
            KR1 = Conductivity.Cells(I + 4, J + 4).Value
            KRT(I, J) = 2 * Pi * KR1 / AA(J)
            KZ1 = Conductivity.Cells(I + 4, J + 4).Value
            KZT(I, J) = 2 * Area(J) * KZ1
        Next
    Next
End If

```

'Loop to set storage and hydraulic conductivity in formation when skin is present
'and have homogeneous formation properties

If ISKIN = 1 And LAYPROP = 1 Then

For I = 1 To Layers

For J = SkinCylinders + 1 To Cylinders

S2(I, J) = DataSheet.Cells(16, 3).Value

KR2 = DataSheet.Cells(14, 3).Value

$KRT(I, J) = 2 * \text{Pi} * KR2 / AA(J)$

KZ2 = DataSheet.Cells(15, 3).Value

$KZT(I, J) = 2 * \text{Area}(J) * KZ2$

Next

Next

End If

'Loop to set storage and hydraulic conductivity in formation when skin is present
'and have heterogeneous formation properties

If ISKIN = 1 And LAYPROP = 0 Then

For I = 1 To Layers

For J = SkinCylinders + 1 To Cylinders

ST2(I) = Worksheets("Layer Properties").Cells(I + 7,
4).Value

S2(I, J) = ST2(I)

KR2AR(I) = Worksheets("Layer Properties").Cells(I + 7,
2).Value

KR2 = KR2AR(FS)

$KRT(I, J) = 2 * \text{Pi} * KR2AR(I) / AA(J)$

KZ2AR(I) = Worksheets("Layer Properties").Cells(I + 7,
3).Value

$KZT(I, J) = 2 * \text{Area}(J) * KZ2AR(I)$

Next

Next

End If

'Set initial head in model

For I = 1 To Layers

For J = 1 To Cylinders

NewHead(I, J) = InitialHead

OldHead(I, J) = InitialHead

Next

Next

'In unconfined model, checking which storage parameter to use

SY1 = DataSheet.Cells(15, 11).Value

SY2 = DataSheet.Cells(17, 3).Value


```

For I = 1 To Layers
  For J = 1 To SkinCylinders
    If NewHead(I, J) < Elevation(I) Then
      Storage(I, J) = SY1
    Else
      Storage(I, J) = S1(I, J) * Thickness(I, J)
    End If
  Next
  For J = SkinCylinders + 1 To Cylinders
    If NewHead(I, J) < Elevation(I) Then
      Storage(I, J) = SY2
    Else
      Storage(I, J) = S2(I, J) * Thickness(I, J)
    End If
  Next
Next

For I = 1 To Layers
  For J = 1 To Cylinders
    Status(I, J) = 1
  Next
Next

Counter = 1
Step = 50

WellFlowVolume = 0
CellFlowVolume = 0

FirstCall = True
RowCounter = 0
WellGradient = 1
Target = 1
AnotherTarget = 1

CumulativeTime = 0

End Sub

```

```
Sub CalculateConductances()
```

```

  Dim UpperThickness As Double
  Dim LowerThickness As Double
  Dim TheThickness As Double
  Dim Bottom As Double

```

```

For I = 1 To Layers
  For J = 1 To Cylinders
    If Status(I, J) <> 0 Then
      Cr(I, J) = KRT(I, J) * Thickness(I, J)

      If I < Layers Then
        Cv(I, J) = (((2 * KZT(I, J) * KZT(I + 1, J)) /
          (KZT(I, J) + KZT(I + 1, J)))) / (Thickness(I + 1, J)
          + Thickness(I, J))
      End If
    End If
  Next
Next

```

End Sub

Sub Reformulate() 'Subroutine to check the status of cells for an unconfined model

```

Dim BottomElevation As Double

For I = 1 To Layers
  If I < Layers Then
    BottomElevation = Elevation(I + 1)
  Else
    BottomElevation = Base
  End If

  For J = 1 To Cylinders
    If Status(I, J) = 1 Then
      If NewHead(I, J) < BottomElevation Then
        Status(I, J) = 0
      End If
    End If

    If I > 1 Then
      If Status(I - 1, J) = 0 Then
        If Status(I, J) = 1 Then
          If NewHead(I, J) > Elevation(I) Then
            Status(I - 1, J) = 1
            NewHead(I - 1, J) = NewHead(I, J)
            NewHead(I, J) = Elevation(I)
            If J <= SkinCylinders Then
              Storage(I - 1, J) = SY1
              Storage(I, J) = S1(I, J) *
                Thickness(I, J)
            End If
          End If
        End If
      End If
    End If
  Next
Next

```

```

Else
    Storage(I - 1, J) = SY2
    Storage(I, J) = S2(I, J) *
    Thickness(I, J)
End If
End If
End If
End If
Next
Next
CalculateConductances 'this could be done within the iteration loop for
                       'greater accuracy, but more computation time

End Sub

```

```

Sub CalculateDimensionlessParameters()

```

```

    DWellHead = (WellHead - InitialHead) / Stress
    DTime = (CumulativeTime * KR2 * B2) / (CasingRadius * CasingRadius) 'we
                                                'use KGS dimensionless parameters

```

```

End Sub

```

```

Sub DetermineWellHead()

```

```

    Dim TemporaryWellGradient As Double
    Dim WellFlow As Double

    If FirstCall Then
        WellHead = StressHead
        FirstCall = False
    Else
        WellFlow = 0

        For I = FS To LS
            WellConductance = KRT(I, 1) * Thickness(I, 1) 'only need to
                                                            'calculate this if thickness may change
            WellFlow = WellFlow + WellConductance * (WellHead -
            OldHead(I, 1))
        Next

        WellHead = WellHead - (WellFlow * Time / ReservoirArea)

```


UpperC) + (Alpha * LowerC)

Old = (1 - Alpha) * ((InnerC * InnerOldHead) - (InnerC *
CenterOldHead) + (OuterC * OuterOldHead) - (OuterC *
CenterOldHead) + (UpperC * UpOldHead) - (UpperC *
CenterOldHead) + (LowerC * DownOldHead) - (LowerC *
CenterOldHead))

Temporary = NewHead(I, J)

NewHead(I, J) = ((D * CenterOldHead) + Old + (InnerC *
Alpha * InnerNewHead) + (OuterC * Alpha *
OuterNewHead) + (UpperC * Alpha * UpNewHead) +
(LowerC * Alpha * DownNewHead)) / E

Error = Abs(NewHead(I, J) - Temporary)

If Error > Maximum Then

Maximum = Error

End If

Next

Next

Iteration = Iteration + 1

Loop

End Sub

Sub GenerateGeometry()

Dim BL As Double

BL = B - B1 - B2 'BL is the thickness of the interval below the screen

FS = NU + 1 'first layer within the screen

LS = NU + NS 'last layer within the screen

Base = 0 'bottom elevation of the first layer; should be read from the data
'sheet and default to 0

If LAYPROP = 1 Then

For J = 1 To Cylinders

For I = 1 To NU

Thickness(I, J) = B1 / NU

Next

For I = FS To LS

Thickness(I, J) = B2 / NS

```

        Next
        For I = LS + 1 To Layers
            Thickness(I, J) = BL / NL
        Next
    Next
End If

If LAYPROP = 0 Then
    For J = 1 To Cylinders
        For I = 1 To NU
            Thickness(I, J) = Worksheets("Layer Properties").Cells(I +
            7, 1).Value
        Next
        For I = FS To LS
            Thickness(I, J) = Worksheets("Layer Properties").Cells(I +
            7, 1).Value
        Next
        For I = LS + 1 To Layers
            Thickness(I, J) = Worksheets("Layer Properties").Cells(I +
            7, 1).Value
        Next
    Next
End If

Elevation(1) = Base + B

For I = 2 To Layers
    Elevation(I) = Elevation(I - 1) - Thickness(I - 1, 1) 'note that the elevations
    'are based on initial thicknesses; thickness
    'may change during a simulation of a test in
    'an unconfined unit
Next

ReservoirArea = CasingRadius * CasingRadius * Pi

Radius(1) = WellRadius + SkinCellWidth
For J = 2 To SkinCylinders
    Radius(J) = Radius(J - 1) + SkinCellWidth
Next

AA(1) = Log(Radius(1)) - Log(WellRadius)
G = Exp(AA(1))

For J = SkinCylinders + 1 To Cylinders
    Radius(J) = Radius(J - 1) * G
Next

```

```

For J = 2 To Cylinders
    AA(J) = Log(Radius(J)) - Log(Radius(J - 1))
Next

Edge(1) = Radius(1) + SkinCellWidth / 2
For J = 2 To SkinCylinders
    Edge(J) = Edge(J - 1) + SkinCellWidth
Next

For J = SkinCylinders + 1 To Cylinders
    Edge(J) = Edge(J - 1) * G
Next

Area(1) = Pi * (Edge(1) * Edge(1) - WellRadius * WellRadius)
For J = 2 To Cylinders
    Area(J) = Pi * (Edge(J) * Edge(J) - Edge(J - 1) * Edge(J - 1))
Next

```

End Sub

Sub aaaMain()

```

InitializeModel
CalculateConductances

Do While WellGradient > Recovery

    DetermineWellHead

    For I = 1 To Layers
        For J = 1 To Cylinders
            OldHead(I, J) = NewHead(I, J)
        Next
    Next

    OldWellHead = WellHead

    'Adding spaces to the arrays if head is still changing in last cylinder

    If ((NewHead(FS, Cylinders) - InitialHead) > 0.00000001) And
        (Cylinders < 200) Then
        Cylinders = Cylinders + 1
        ReDim Preserve NewHead(1 To Layers, 1 To Cylinders)
        ReDim Preserve OldHead(1 To Layers, 1 To Cylinders)
    End If

```

ReDim Preserve Thickness(1 To Layers, 1 To Cylinders)
 ReDim Preserve Status(1 To Layers, 1 To Cylinders)
 ReDim Preserve Storage(1 To Layers, 1 To Cylinders)
 ReDim Preserve S1(1 To Layers, 1 To Cylinders)
 ReDim Preserve S2(1 To Layers, 1 To Cylinders)
 ReDim Preserve KRT(1 To Layers, 1 To Cylinders)
 ReDim Preserve KZT(1 To Layers, 1 To Cylinders)

ReDim Preserve Cr(1 To Layers, 1 To Cylinders)
 ReDim Preserve Cv(1 To Layers, 1 To Cylinders)

ReDim Preserve Radius(1 To Cylinders)
 ReDim Preserve AA(1 To Cylinders)
 ReDim Preserve Area(1 To Cylinders)

$Radius(Cylinders) = Radius(Cylinders - 1) * G$
 $AA(Cylinders) = Log(Radius(Cylinders)) - Log(Radius(Cylinders - 1))$
 $Area(Cylinders) = Pi * (Radius(Cylinders) * Radius(Cylinders) - Radius(Cylinders - 1) * Radius(Cylinders - 1))$

For I = 1 To NU
 Thickness(I, Cylinders) = Thickness(I, Cylinders - 1)
 Next

For I = NU + 1 To NU + NS
 Thickness(I, Cylinders) = Thickness(I, Cylinders - 1)
 Next

For I = NU + NS + 1 To NU + NS + NL
 Thickness(I, Cylinders) = Thickness(I, Cylinders - 1)
 Next

For I = 1 To Layers
 NewHead(I, Cylinders) = InitialHead
 OldHead(I, Cylinders) = InitialHead
 Status(I, Cylinders) = 1
 Storage(I, Cylinders) = S2(I, J)
 KRT(I, Cylinders) = 2 * Pi * KR2 / AA(Cylinders)
 KZT(I, Cylinders) = 2 * Area(Cylinders) * KZ2
 Cr(I, Cylinders) = KRT(I, Cylinders) * Thickness(I, Cylinders)

If I < Layers Then
 Cv(I, J) = KZT(I, Cylinders) / (Thickness(I + 1,


```

                Cylinders) + Thickness(I, Cylinders))
            End If
        Next
    End If

    GaussSeidel
    DisplayProgress

    CumulativeTime = CumulativeTime + Time

    For I = 1 To Layers
        For J = 1 To Cylinders
            CellFlowVolume = CellFlowVolume + Storage(I, J) *
                (NewHead(I, J) - OldHead(I, J)) * Area(J)
        Next
    Next

    If Confined = 2 Then
        Reformulate 'this needs to be turned on for unconfined cases only
    End If

    'adjust the time step based on the change in well gradient at the start of
    'each time steps
    If (Difference < 0.000004) Then
        Time = Time * 1.005
    End If

    If (Difference > 0.000004) Then
        Time = Time / 1.005
    End If

    CalculateDimensionlessParameters

    If WellGradient <= Target Then
        PrintHeads
        Target = Target - 0.01
    End If

    If (DWellHead <= AnotherTarget) And (DWellHead < 0.99) Then
        PrintWelleffects
        AnotherTarget = AnotherTarget - 0.01
    End If

    If Counter = Step Then
        Counter = 0
    End If

```

```
Counter = Counter + 1
```

```
Loop
```

```
'calculate a budget
```

```
Results.Cells(1, 10).Value = CellFlowVolume
```

```
Results.Cells(2, 10).Value = WellFlowVolume
```

```
For J = 1 To Cylinders
```

```
    Results.Cells(J, 6).Value = Radius(J)
```

```
Next
```

```
For I = 1 To Layers
```

```
    For J = 1 To Cylinders
```

```
        Worksheets("Aquifer Heads").Cells(I, J).Value = NewHead(I, J)
```

```
    Next
```

```
Next
```

```
End Sub
```

```
Sub PrintHeads()
```

```
    If Cylinders < 100 Then
```

```
        Index = Cylinders
```

```
    Else
```

```
        Index = 100
```

```
    End If
```

```
    For J = 1 To Cylinders
```

```
        Results.Cells(J, 2).Value = NewHead(FS, J)
```

```
    Next
```

```
End Sub
```

```
Sub PrintWellEffects()
```

```
    RowCounter = RowCounter + 1
```

```
    Results.Cells(RowCounter, 3).Value = CumulativeTime
```

```
    Results.Cells(RowCounter, 4).Value = DTime
```

```
    Results.Cells(RowCounter, 5).Value = DWellHead
```

```
Worksheets("Field Analysis").Cells(RowCounter, 1).Value = CumulativeTime
Worksheets("Field Analysis").Cells(RowCounter, 2).Value = DWellHead
```

```
End Sub
```

```
Sub SetHeads()
```

```
    InnerC = Cr(I, J)
    If J = 1 Then
        If I >= FS And I <= LS Then
            InnerNewHead = WellHead 'this is only true if we are in the well
                                   'screen
            InnerOldHead = OldWellHead
        Else
            InnerC = 0 'outside the screen, inner radial conductance is 0
        End If
    Else
        InnerNewHead = NewHead(I, J - 1)
        InnerOldHead = OldHead(I, J - 1)
    End If

    If J < Cylinders Then
        OuterNewHead = NewHead(I, J + 1)
        OuterOldHead = OldHead(I, J + 1)
        OuterC = Cr(I, J + 1)
    Else
        OuterC = 0
    End If

    If I > 1 Then
        UpNewHead = NewHead(I - 1, J)
        UpOldHead = OldHead(I - 1, J)
        UpperC = Cv(I - 1, J)
    Else
        UpperC = 0
    End If

    If I < Layers Then
        DownNewHead = NewHead(I + 1, J)
        DownOldHead = OldHead(I + 1, J)
        LowerC = Cv(I, J)
    Else
        LowerC = 0
    End If
```

End Sub

Sub WellSkinOption()

Dim I As Long

Dim Condition As Boolean

Condition = Worksheets("Data Entry").Cells(2, 50)

Worksheets("Data Entry").Unprotect

For I = 12 To 15

 If Condition = False Then

 Worksheets("Data Entry").Cells(I, 11).Interior.Color = 16776960

 Else

 Worksheets("Data Entry").Cells(I, 11).Interior.Color = 16777215

 End If

Next

Worksheets("Data Entry").Protect

End Sub

Sub HomogeneousOption()

Dim I As Long

Dim Condition As Boolean

Condition = Worksheets("Data Entry").Cells(3, 50)

Worksheets("Data Entry").Unprotect

For I = 19 To 20

 If Condition = False Then

 Worksheets("Data Entry").Cells(I, 11).Interior.Color = 16776960

 Else

 Worksheets("Data Entry").Cells(I, 11).Interior.Color = 16777215

 End If

Next

Worksheets("Data Entry").Protect

End Sub

```
Sub LayerPropertyOption()  
  
    Dim I As Long  
    Dim Condition As Boolean  
  
    Condition = Worksheets("Data Entry").Cells(4, 50)  
    Worksheets("Data Entry").Unprotect  
  
    For I = 14 To 16  
        If Condition = False Then  
            Worksheets("Data Entry").Cells(I, 3).Interior.Color = 16776960  
        Else  
            Worksheets("Data Entry").Cells(I, 3).Interior.Color = 16777215  
        End If  
    Next  
  
    Worksheets("Data Entry").Protect  
  
End Sub
```

APPENDIX B

DPPS Visual Basic Code

Option Explicit

Public Const Pi As Double = 3.14159265358979

Public NewHead() As Double

Public OldHead() As Double

Public Radius() As Double

Public Edge() As Double 'only used for the block-centered approach

Public Volume() As Double

Public Area() As Double

Public Thickness() As Double

Public Elevation() As Double

Public Status() As Long

Public Recharge() As Double

Public Base As Double 'the elevation of the bottom of the flow system

Public KRT() As Double

Public KZT() As Double

Public KR1 As Double

Public KZ1 As Double

Public KR2 As Double

Public KZ2 As Double

Public Storage() As Double

Public Q As Double

Public InitialHead As Double

Public WellHead As Double

Public OldWellHead As Double

Public DWellHead As Double

Public CumulativeTime As Double

Public Tolerance As Double

Public Maximum As Double

Public Stress As Double

Public StressHead As Double

Public ReservoirArea As Double

Public WellConductance As Double

Public Gradient As Double

Public AA() As Double

Public CasingRadius As Double

Public WellRadius As Double

Public Time As Double

Public TestTime As Single

Public Multiplier As Single
Public NumTimeSteps As Single
Public DTime As Double
Public Target As Double
Public AnotherTarget As Double
Public Difference As Double
Public Alpha As Double
Public G As Double
Public PerComp As Double

Public i As Long
Public j As Long
Public Layers As Long
Public Cylinders As Long
Public SkinCylinders As Long

Public SkinRadius As Double
Public SkinCellWidth As Double 'this is a uniform number for each cell in the skin
Public Index As Long
Public Counter As Long
Public Step As Long
Public Iteration As Long

Public FirstCall As Boolean

Public Cr() As Double
Public Cv() As Double

Public Ktype As Double

Public B As Double
Public B1 As Double
Public B2 As Double
Public B3 As Double
Public B4 As Double
Public SL As Long
Public NAT As Long
Public NBT As Long
Public NAS As Long
Public NS As Long
Public NBS As Long
Public S1 As Double
Public S2 As Double
Public Sy1 As Double
Public Sy2 As Double
Public UpperInterval As Long

Public LowerInterval As Long

Public RowCounter As Long

Public Old As Double

Public Error As Double

Public InnerOldHead As Double

Public OuterOldHead As Double

Public InnerNewHead As Double

Public OuterNewHead As Double

Public UpOldHead As Double

Public DownOldHead As Double

Public UpNewHead As Double

Public DownNewHead As Double

Public CenterOldHead As Double

Public Temporary As Double

Public D As Double

Public E As Double

Public InnerC As Double

Public OuterC As Double

Public UpperC As Double

Public LowerC As Double

Public Confined As Integer

Public Skin As Boolean

Public Homogeneous As Boolean

Public ISKIN As Long

Public HOMOSKIN As Long

Public DataSheet As Worksheet

Public Results As Worksheet

Public Conductivity As Worksheet

Sub InitializeModel()

'Set the names of the sheets that will be used for input/output

Set DataSheet = Worksheets("Data Entry")

Set Results = Worksheets("Well Results")

Set Conductivity = Worksheets("Conductivity")

'Set model geometry

CasingRadius = DataSheet.Cells(5, 3)

WellRadius = DataSheet.Cells(6, 3).Value

Cylinders = DataSheet.Cells(7, 3).Value

'Set formation parameters

B = DataSheet.Cells(12, 3).Value 'total thickness

S2 = DataSheet.Cells(15, 3).Value

Q = DataSheet.Cells(22, 3)

InitialHead = DataSheet.Cells(23, 3).Value

'Set DPP screen characteristics

B1 = ((DataSheet.Cells(31, 11).Value) - 0.0125) 'Depth from top of aquifer to
'the upper transducer

B2 = 0.275

B3 = 0.15

B4 = B - B1 - B2 - B3

NAT = B1 / 0.03 'Number of layers above upper transducer

NBT = 10 'Number of layers between transducers

NAS = 5 'Number of layers above DPP screen

NS = 1 'Number of DPP screen layers

NBS = B4 / 0.03 'Number of layers below DPP screen

Layers = NAT + NBT + NAS + NS + NBS

'Setting the size of all of the arrays

ReDim Radius(1 To Cylinders)

ReDim Edge(1 To Cylinders)

ReDim NewHead(1 To Layers, 1 To Cylinders)

ReDim OldHead(1 To Layers, 1 To Cylinders)

ReDim Thickness(1 To Layers, 1 To Cylinders)

ReDim Elevation(1 To Layers)

ReDim Volume(1 To Layers, 1 To Cylinders)

ReDim Status(1 To Layers, 1 To Cylinders)

ReDim Recharge(1 To Layers, 1 To Cylinders)

ReDim Cr(1 To Layers, 1 To Cylinders)

ReDim Cv(1 To Layers, 1 To Cylinders)

ReDim Area(1 To Cylinders)

ReDim AA(1 To Cylinders)

ReDim KRT(1 To Layers, 1 To Cylinders)

ReDim KZT(1 To Layers, 1 To Cylinders)

ReDim Storage(1 To Layers, 1 To Cylinders)

'Setting the values of the check buttons/boxes

Confined = DataSheet.Cells(1, 50).Value

Skin = DataSheet.Cells(2, 50).Value

Homogeneous = DataSheet.Cells(3, 50).Value

If Skin Then ISKIN = 1 Else ISKIN = 0

If Homogeneous Then HOMOSKIN = 1 Else HOMOSKIN = 0

'Set time variables

TestTime = DataSheet.Cells(28, 3).Value

Multiplier = DataSheet.Cells(29, 3).Value

NumTimeSteps = DataSheet.Cells(30, 3).Value

If Multiplier = 1 Then

 Time = TestTime / NumTimeSteps

Else

 Time = (TestTime * (1 - Multiplier)) / (1 - Multiplier ^ NumTimeSteps)

End If

'Set model variables

Tolerance = DataSheet.Cells(25, 11).Value

Alpha = DataSheet.Cells(26, 11).Value

'If user inputs no skin, then for code to work, we are setting 1 skin cell with the
'same hydraulic conductivity as formation in order to set locations of
'corresponding nodes

If ISKIN = 0 Then

 SkinCylinders = 1

 SkinCellWidth = 0.01

Else

 SkinRadius = DataSheet.Cells(12, 11).Value

 SkinCylinders = DataSheet.Cells(13, 11).Value

 SkinCellWidth = (SkinRadius - WellRadius) / SkinCylinders

End If

S1 = DataSheet.Cells(14, 11).Value

GenerateGeometry

'Loop to set storage and hydraulic conductivity if no skin present

If ISKIN = 0 Then

 For i = 1 To Layers

 For j = 1 To Cylinders

 S1 = S2

 KR2 = DataSheet.Cells(13, 3).Value

 KR1 = KR2

 KRT(i, j) = 2 * Pi * KR2 / AA(j)

 KZ2 = DataSheet.Cells(14, 3).Value

```

        KZ1 = KZ2
        KZT(i, j) = 2 * Area(j) * KZ2
    Next
Next
End If

'Loop to set hydraulic conductivity in skin when skin is present
If ISKIN = 1 And HOMOSKIN = 1 Then
    For i = 1 To Layers
        For j = 1 To SkinCylinders
            KR1 = DataSheet.Cells(19, 11).Value
            KRT(i, j) = 2 * Pi * KR1 / AA(j)
            KZ1 = DataSheet.Cells(20, 11).Value
            KZT(i, j) = 2 * Area(j) * KZ1
        Next
    Next
End If

If ISKIN = 1 And HOMOSKIN = 0 Then
    For i = 1 To Layers
        For j = 1 To SkinCylinders
            KR1 = Conductivity.Cells(i + 4, j + 4).Value
            KRT(i, j) = 2 * Pi * KR1 / AA(j)
            KZ1 = Conductivity.Cells(i + 4, j + 4).Value
            KZT(i, j) = 2 * Area(j) * KZ1
        Next
    Next
End If

'Loop to set hydraulic conductivity in formation when skin is present
If ISKIN = 1 Then
    For i = 1 To Layers
        For j = SkinCylinders + 1 To Cylinders
            KR2 = DataSheet.Cells(13, 3).Value
            KRT(i, j) = 2 * Pi * KR2 / AA(j)
            KZ2 = DataSheet.Cells(14, 3).Value
            KZT(i, j) = 2 * Area(j) * KZ2
        Next
    Next
End If

For i = 1 To Layers
    For j = 1 To Cylinders
        NewHead(i, j) = InitialHead
        OldHead(i, j) = InitialHead
    Next

```

Next

'In unconfined model, checking which storage parameter to use

Sy1 = DataSheet.Cells(15, 11).Value

Sy2 = DataSheet.Cells(16, 3).Value

For i = 1 To Layers

 For j = 1 To SkinCylinders

 If NewHead(i, j) < Elevation(i) Then

 Storage(i, j) = Sy1

 Else

 Storage(i, j) = S1 * Thickness(i, j)

 End If

 Next

 For j = SkinCylinders + 1 To Cylinders

 If NewHead(i, j) < Elevation(i) Then

 Storage(i, j) = Sy2

 Else

 Storage(i, j) = S2 * Thickness(i, j)

 End If

 Next

Next

For i = 1 To Layers

 For j = 1 To Cylinders

 Status(i, j) = 1

 Next

Next

Time = (TestTime * (1 - Multiplier)) / (1 - Multiplier ^ NumTimeSteps)

Counter = 1

Step = 50

FirstCall = True

RowCounter = 0

Target = 1

AnotherTarget = 1

CumulativeTime = 0

Set_Recharge

End Sub

```
Sub Set_Recharge()
```

```
    'Initialize recharge everywhere to zero
```

```
    For i = 1 To Layers
```

```
        For j = 1 To Cylinders
```

```
            Recharge(i, j) = 0
```

```
        Next
```

```
    Next
```

```
    'Set boundary conditions at DPP screen
```

```
    SL = NAT + NBT + NAS + NS
```

```
    Recharge(SL, 1) = Q
```

```
End Sub
```

```
Sub CalculateConductances()
```

```
    Dim UpperThickness As Double
```

```
    Dim LowerThickness As Double
```

```
    Dim TheThickness As Double
```

```
    Dim Bottom As Double
```

```
    For i = 1 To Layers
```

```
        For j = 1 To Cylinders
```

```
            If Status(i, j) <> 0 Then
```

```
                Cr(i, j) = KRT(i, j) * Thickness(i, j)
```

```
                If i < Layers Then
```

```
                    Cv(i, j) = (((2 * KZT(i, j) * KZT(i + 1, j)) / (KZT(i, j) + KZT(i + 1, j)))) / (Thickness(i + 1, j) + Thickness(i, j))
```

```
                End If
```

```
            End If
```

```
        Next
```

```
    Next
```

```
End Sub
```

```
Sub Reformulate() 'Subroutine to check the status of cells for an unconfined model
```

```
    Dim BottomElevation As Double
```

```
    For i = 1 To Layers
```

```
        If i < Layers Then
```

```
            BottomElevation = Elevation(i + 1)
```

```

Else
    BottomElevation = Base
End If
For j = 1 To Cylinders
    If Status(i, j) = 1 Then
        If NewHead(i, j) < BottomElevation Then 'turn this cell off
            Status(i, j) = 0
        End If
    End If
    If i > 1 Then
        If Status(i - 1, j) = 0 Then
            If Status(i, j) = 1 Then
                If NewHead(i, j) > Elevation(i) Then
                    Status(i - 1, j) = 1
                    NewHead(i - 1, j) = NewHead(i, j)
                    NewHead(i, j) = Elevation(i)
                    If j <= SkinCylinders Then
                        Storage(i - 1, j) = Sy1
                        Storage(i, j) = S1 *
                            Thickness(i, j)
                    Else
                        Storage(i - 1, j) = Sy2
                        Storage(i, j) = S2 *
                            Thickness(i, j)
                    End If
                End If
            End If
        End If
    End If
End If
Next
Next

CalculateConductances    'this could be done within the iteration loop for
                          'greater accuracy, but more computation time

End Sub

```

```

Sub DisplayProgress()

```

```

    Worksheets("Data Entry").Unprotect

    If Counter = Step Then
        DataSheet.Cells(5, 15).Value = CumulativeTime
    End If

```

Worksheets("Data Entry").Protect

End Sub

Sub GaussSeidel()

Maximum = Tolerance + 1

Iteration = 0

Do While Maximum > Tolerance

Maximum = 0

For i = 1 To Layers

For j = 1 To Cylinders

SetHeads

CenterOldHead = OldHead(i, j)

D = Storage(i, j) * Area(j) / Time

E = D + (Alpha * InnerC) + (Alpha * OuterC) + (Alpha *
UpperC) + (Alpha * LowerC)

Old = (1 - Alpha) * ((InnerC * InnerOldHead) - (InnerC *
CenterOldHead) + (OuterC * OuterOldHead) - (OuterC *
CenterOldHead) + (UpperC * UpOldHead) - (UpperC *
CenterOldHead) + (LowerC * DownOldHead) - (LowerC *
CenterOldHead))

Temporary = NewHead(i, j)

NewHead(i, j) = ((D * CenterOldHead) + Old + (InnerC *
Alpha * InnerNewHead) + (OuterC * Alpha *
OuterNewHead) + (UpperC * Alpha * UpNewHead) +
(LowerC * Alpha * DownNewHead) + Recharge(i, j)) / E

Error = Abs(NewHead(i, j) - Temporary)

If Error > Maximum Then

Maximum = Error

End If

Next

Next

Iteration = Iteration + 1

Loop

End Sub

```

Next
For j = 2 To Cylinders
    AA(j) = Log(Radius(j)) - Log(Radius(j - 1))
Next

Edge(1) = Radius(1) + SkinCellWidth / 2
For j = 2 To SkinCylinders
    Edge(j) = Edge(j - 1) + SkinCellWidth
Next

For j = SkinCylinders + 1 To Cylinders
    Edge(j) = Edge(j - 1) * G
Next

Area(1) = Pi * (Edge(1) * Edge(1) - WellRadius * WellRadius)
For j = 2 To Cylinders
    Area(j) = Pi * ((Edge(j) * Edge(j)) - (Edge(j - 1) * Edge(j - 1)))
Next

End Sub

```

```

Sub aaaMain()

```

```

    InitializeModel
    CalculateConductances    'if you do not have an unconfined model,
                            'conductance is constant

    Do While CumulativeTime <= TestTime

        For i = 1 To Layers
            For j = 1 To Cylinders
                OldHead(i, j) = NewHead(i, j)
            Next
        Next

        GaussSeidel
        DisplayProgress

        CumulativeTime = CumulativeTime + Time
        Time = Time * Multiplier

        If Confined = 2 Then
            Reformulate    'this needs to be turned on for unconfined cases only
        End If
    End While
End Sub

```

```

        PrintWellEffects

        If Counter = Step Then
            Counter = 0
        End If

        Counter = Counter + 1
    Loop

    PrintHeads

    For j = 1 To Cylinders
        Results.Cells(j, 4).Value = Radius(j)
    Next

End Sub

```

```

Sub PrintHeads()

    For i = 1 To Layers
        For j = 1 To Cylinders
            Results.Cells(j, 3).Value = NewHead(i, j)
        Next
    Next

    Results.Cells(1, 2).Value = NewHead(NAS + 1, 1)
    Results.Cells(2, 2).Value = NewHead(UpperInterval, 1)

End Sub

```

```

Sub PrintWellEffects()

    RowCounter = RowCounter + 1

End Sub

```

```

Sub SetHeads()

    If j > 1 Then
        InnerNewHead = NewHead(i, j - 1)
        InnerOldHead = OldHead(i, j - 1)
    End If

```

```

        InnerC = Cr(i, j)
    Else
        InnerC = 0 'outside the screen, inner radial conductance is 0
    End If

```

```

If j < Cylinders Then
    OuterNewHead = NewHead(i, j + 1)
    OuterOldHead = OldHead(i, j + 1)
    OuterC = Cr(i, j + 1)
Else
    OuterC = 0
End If

```

```

If i > 1 Then
    UpNewHead = NewHead(i - 1, j)
    UpOldHead = OldHead(i - 1, j)
    UpperC = Cv(i - 1, j)
Else
    UpperC = 0
End If

```

```

If i < Layers Then
    DownNewHead = NewHead(i + 1, j)
    DownOldHead = OldHead(i + 1, j)
    LowerC = Cv(i, j)
Else
    LowerC = 0
End If

```

```
End Sub
```

```
Sub WellSkinOption()
```

```

    Dim i As Long
    Dim Condition As Boolean

```

```

    Condition = Worksheets("Data Entry").Cells(2, 50)
    Worksheets("Data Entry").Unprotect

```

```

For i = 12 To 15
    If Condition = False Then
        Worksheets("Data Entry").Cells(i, 11).Interior.Color = RGB(255,
        100, 100)
    Else
        Worksheets("Data Entry").Cells(i, 11).Interior.Color = 16777215
    End If
Next i

```

```
        End If
    Next

    Worksheets("Data Entry").Protect

End Sub
```

```
Sub HomogeneousOption()

    Dim i As Long
    Dim Condition As Boolean

    Condition = Worksheets("Data Entry").Cells(3, 50)
    Worksheets("Data Entry").Unprotect

    For i = 19 To 20
        If Condition = False Then
            Worksheets("Data Entry").Cells(i, 11).Interior.Color = RGB(255,
            100, 100)
        Else
            Worksheets("Data Entry").Cells(i, 11).Interior.Color = 16777215
        End If
    Next

    Worksheets("Data Entry").Protect

End Sub
```

VITA

Graduate School

Southern Illinois University

John E. Keller

Date of Birth: July 18, 1973

246 Pine Shore Drive, Apt #50, Carbondale, Illinois 62902

University of Kansas

Bachelor of Science, Geology, May 1996

Southern Illinois University at Carbondale

Master of Science, Hydrogeology, December 2000

Dissertation Title:

Accurate Cylindrical-Coordinate Numerical Models for the Analysis of
Hydrologic Tests

Major Professor: Steven P. Esling

Publications:

Esling, Steven P. and Keller, John E., 2009, Design of a user interface for
the Kansas Geological Survey Analytical Model. *Ground Water* 47(4): 587-590.

Esling, Steven P., Keller, John E., and Miller, Kenneth J., 2008, Reducing
Capture Zone Uncertainty with a Systematic Sensitivity Analysis. *Ground Water*
46(4): 570-578.